Article

Unravelling the collateral damage of antibiotics on gut bacteria

https://doi.org/10.1038/s41586-021-03986-2

Received: 6 November 2019

Accepted: 1 September 2021

Lisa Maier[1,2,3,15]✉, Camille V. Goemans[1,15], Jakob Wirbel[4], Michael Kuhn[4], Claudia Eberl[5,6], Mihaela Pruteanu[1,12], Patrick Müller[2,3], Sarela Garcia-Santamarina[1], Elisabetta Cacace[1], Boyao Zhang[4], Cordula Gekeler[2,3], Tisya Banerjee[1,13], Exene Erin Anderson[1,14], Alessio Milanese[4], Ulrike Löber[7,8], Sofia K. Forslund[4,7,8], Kiran Raosaheb Patil[4,9], Michael Zimmermann[4], Bärbel Stecher[5,6], Georg Zeller[4], Peer Bork[4,8,10,11] & Athanasios Typas[1,4]✉

Antibiotics are used to fight pathogens but also target commensal bacteria, disturbing the composition of gut microbiota and causing dysbiosis and disease[1]. Despite this well-known collateral damage, the activity spectrum of different antibiotic classes on gut bacteria remains poorly characterized. Here we characterize further 144 antibiotics from a previous screen of more than 1,000 drugs on 38 representative human gut microbiome species[2]. Antibiotic classes exhibited distinct inhibition spectra, including generation dependence for quinolones and phylogeny independence for β-lactams. Macrolides and tetracyclines, both prototypic bacteriostatic protein synthesis inhibitors, inhibited nearly all commensals tested but also killed several species. Killed bacteria were more readily eliminated from in vitro communities than those inhibited. This species-specific killing activity challenges the long-standing distinction between bactericidal and bacteriostatic antibiotic classes and provides a possible explanation for the strong effect of macrolides on animal[3–5] and human[6,7] gut microbiomes. To mitigate this collateral damage of macrolides and tetracyclines, we screened for drugs that specifically antagonized the antibiotic activity against abundant *Bacteroides* species but not against relevant pathogens. Such antidotes selectively protected *Bacteroides* species from erythromycin treatment in human-stool-derived communities and gnotobiotic mice. These findings illuminate the activity spectra of antibiotics in commensal bacteria and suggest strategies to circumvent their adverse effects on the gut microbiota.

Medication is emerging as a major factor influencing the composition of the human gut microbiota [2,8–10]. Although the role of non-antibiotic drugs has been, until recently, unappreciated [2,10,11], antibiotics developed to have broad-spectrum activities are known to also directly affect gut microbiota. As consequence, they cause many gastrointestinal side effects[12], including *Clostridioides difficile* infections. This collateral damage of antibiotics on the gut microbiota has recently received more attention. In vivo studies have highlighted links between antibiotic-induced long-term microbiota changes and various allergic, metabolic, immunological and inflammatory malfunctions[3–7,13,14]. However, technical difficulties hamper routine testing of antibiotic susceptibility in anaerobic bacteria[15], and available data on bacterial susceptibility to antibiotics offer minimal resolution on human gut bacteria [16]. Information is missing even for common or disease-associated[17,18] gut species. In addition, animal or cohort studies use few antibiotics or merge data on different antibiotic classes, precluding systematic conclusions on antibiotic collateral damage on gut commensals.

We previously assessed the direct effect of 1,197 pharmaceuticals on the growth of 38 prevalent and abundant human-gut-derived bacterial species at a concentration of 20 μM (ref. [2]). A single wild-type strain was used per species, except for *Escherichia coli* and *Bacteroides fragilis*, for which two strains were screened (Supplementary Table 1); unless otherwise mentioned, these are also the strains used here when referring to the species. This initial screen (hereafter called 'screen') included 144 antibiotics with discernible class-dependent effects on gut bacteria (Fig. 1a, Extended Data Fig. 1, Supplementary Table 2). We validated these results by measuring 815 minimal inhibitory concentrations (MICs) for up to 33 antibiotics and two antifungals across

---

[1]Genome Biology Unit, European Molecular Biology Laboratory, Heidelberg, Germany. [2]Interfaculty Institute of Microbiology and Infection Medicine, University of Tübingen, Tübingen, Germany. [3]Cluster of Excellence 'Controlling Microbes to Fight Infections', University of Tübingen, Tübingen, Germany. [4]Structural and Computational Biology Unit, European Molecular Biology Laboratory, Heidelberg, Germany. [5]Max-von-Pettenkofer Institute, LMU Munich, Munich, Germany. [6]German Center for Infection Research (DZIF), partner site LMU Munich, Munich, Germany. [7]Experimental and Clinical Research Center, a cooperation of Charité - Universitätsmedizin Berlin and Max-Delbrück-Center for Molecular Medicine, Berlin, Germany. [8]Max-Delbrück-Center for Molecular Medicine, Berlin, Germany. [9]The Medical Research Council Toxicology Unit, University of Cambridge, Cambridge, UK. [10]Yonsei Frontier Lab (YFL), Yonsei University, Seoul, South Korea. [11]Department of Bioinformatics, Biocenter, University of Würzburg, Würzburg, Germany. [12]Present address: Department of Biology, Humboldt University Berlin, Berlin, Germany. [13]Present address: Department of Chemistry, TU Munich, Munich, Germany. [14]Present address: NYU School of Medicine, New York, NY, USA. [15]These authors contributed equally: Lisa Maier, Camille V. Goemans. ✉e-mail: l.maier@uni-tuebingen.de; typas@embl.de

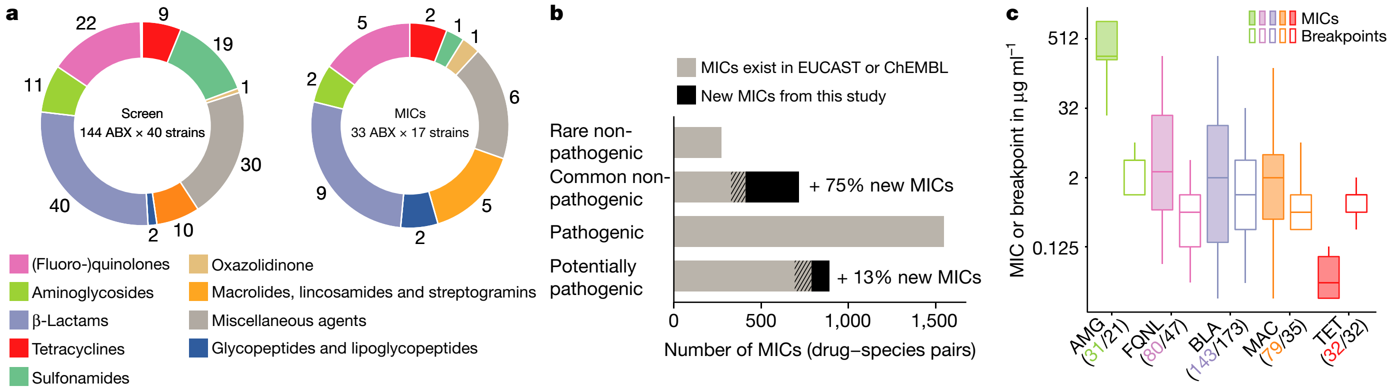

Fig 1 | Activity spectrum of antibiotic classes on human gut commensals. **a**, Overview of antibiotics tested in initial screen at 20 μM concentration[2] and validated by MIC determination in this study. **b**, Comparison of measured MICs (dark grey) to available ones from public databases (light grey). Shaded areas represent the overlap. Species are classified as 'common' if they are present in the gut microbiome of more than 1% of 727 healthy individuals. **c**, MICs of drug–species pairs per antibiotic class (colour scheme as in **a**) are depicted next to EUCAST clinical (susceptibility) breakpoints for pathogens. Numbers of drug–species pairs (MICs; coloured) and antibiotic per class (EUCAST clinical breakpoints; black) are shown in parentheses. Boxes span the interquartile range (IQR), and whiskers extend to the most extreme data points up to a maximum of 1.5× IQR. The *y* axis is $\log_2$ scale.

16 strains from the screen and 11 additional ones to account better for intra- and interspecies variation within the *Bacteroides* genus (Extended Data Fig. 2, Supplementary Tables 3, 4). Despite experimental differences, the screen exhibited high specificity and sensitivity when benchmarked against the MIC data (Extended Data Fig. 3a). The measured MICs also correlated well with the limited available data on antimicrobial susceptibility from EUCAST[16] or ChEMBL[19] ($r_s = 0.70$ and $r_s = 0.64$; $n = 77$ and $n = 132$, respectively), despite differences in strains and media used (Extended Data Fig. 3b). Importantly, this dataset expands the available MICs, up to 75% for non-pathogenic bacteria (Fig. 1b, Extended Data Fig. 3c). Altogether, the screen and MIC dataset provide high-resolution information on the target spectrum of antibiotics on commensal bacteria.

Antibiotic classes exhibited distinct behaviours (Extended Data Fig. 4a). For example, quinolones acted according to their generation. First-generation variants were effective against few bacterial species; second- and third-generation quinolones had broader activity; and fourth-generation variants (developed to increase activity against anaerobes) inhibited almost all tested species (Extended Data Fig. 4b). For β-lactams, resistance was phylogenetically patchy, which was corroborated by additional data collected for *Bacteroides* strains and species (Extended Data Figs. 2, 4c–e). β-Lactam sensitivity and phylogenetic relatedness within the *Bacteroides* genus were uncoupled (Extended Data Fig. 4e). This implies that β-lactam resistance mechanisms are strain specific and horizontally transferred. Macrolides showed a strong effect on gut commensals and inhibited all tested microorganisms (Extended Data Fig. 4a), except for *C. difficile*, which was resistant to macrolides and clindamycin (Extended Data Fig. 2, red box), consistent with the known risk of *C. difficile* infection after macrolide or clindamycin treatment[20]. Finally, 8 out of 9 tested tetracyclines inhibited nearly all tested species, which is surprising because the gut microbiota has been considered as a reservoir for tetracycline-resistance genes[21]. Concentration-resolved MICs confirmed the drug class-dependent trends observed in the screen. In addition, MICs allowed for comparisons with clinical breakpoints—that is, MICs below which a species is considered susceptible (Fig. 1c). Overall, the gut commensal bacteria studied here (anaerobic growth, modified GAM broth[22]) had slightly higher MICs than those reported for pathogens (aerobic growth, Mueller–Hinton agar). Tetracyclines were the exception, inhibiting commensals at significantly lower concentrations (Fig. 1c).

Recent in vivo studies have shown that β-lactams and macrolides can strongly affect the gut microbiota and, thereby, the health of the host[3–5]. As β-lactams exhibited strain-specific activity and are known to kill bacteria (bactericidal), we reasoned that they would irrevocably deplete specific microbiota members and, hence, cause long-lasting effects on community composition. By contrast, macrolides affected all tested gut commensals and are textbook bacteriostatic antibiotics—that is, they inhibit bacterial growth but do not kill (at high numbers). Hence, the long-term community composition change is harder to rationalize, as all community members would be uniformly inhibited but should regrow once treatment stops. Similarly, bacteriostatic tetracyclines acted across the board and have known gastrointestinal side effects[12], which are indicative of perturbed gut microbiota. We thus wondered at which level macrolides and tetracyclines act differently on gut bacteria. Although both clinical use[23,24] and basic research[25] rely heavily on classifying antibiotic classes as bactericidal or bacteriostatic, there are reports of antibiotics changing killing capacities depending on the organism, drug concentration or medium tested[26,27] (and meta-analyses indicating that the distinction has little relevance to clinical practice[28,29]). We hypothesized that this bacteriostatic–bactericidal divide might be less rigid for gut commensals, because they represent more phylogenetic diversity than the few pathogens usually tested for antibiotic susceptibility.

The standard way to determine whether antibiotics are bactericidal is to perform time kill assays, in which survival is counted on agar (forming colonies) after drug treatment. If, over a period of antibiotic treatment (5–24 h) at concentrations above MIC, the number of colony forming units (CFU) per ml decreases by more than 99.9%, the antibiotic is considered bactericidal[26]. We assessed the survival of 12 abundant gut bacteria over a 5-h treatment with a macrolide (erythromycin or azithromycin) or a tetracycline (doxycycline) at 5× MIC (Fig 2a, Extended Data Fig. 5a). In nearly half of the cases, survival decreased (rapidly) by more than 99.9%, indicating that these drugs are bactericidal to several abundant gut commensals. This was corroborated by testing the viability of *Bacteroides vulgatus* and *E. coli* ED1a upon erythromycin, azithromycin or doxycycline treatment with microscopy and flow cytometry (Extended Data Fig. 5b). We excluded that differences in killing capacity were confounded by growth rate, growth phase or MIC and established that active growth was needed for almost all cases of killing (Extended Data Fig. 6). Interestingly, *B. vulgatus* and *Bacteroides uniformis* cultures lysed when treated with erythromycin (Fig. 2b), as confirmed by time-lapse microscopy, with erythromycin causing cell shape defects and ultimately lysing both species (Fig. 2c, Supplementary Videos 1–4). As tetracyclines are established bacteriostatic drugs in *E. coli*, we were surprised to see that doxycycline killed

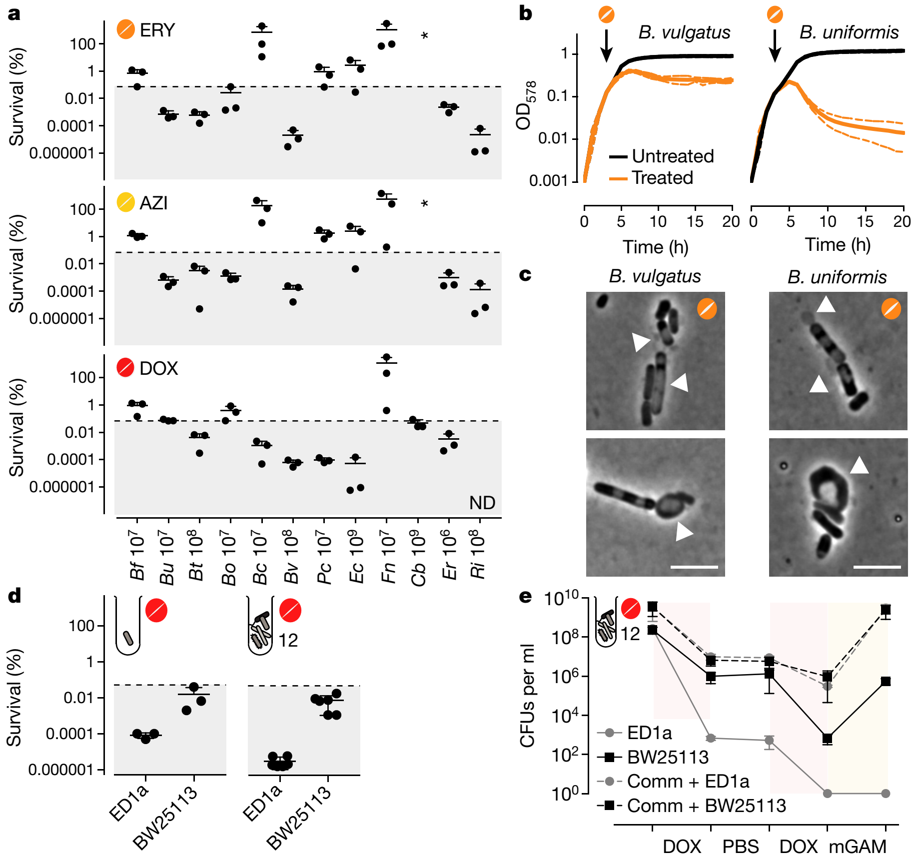

Fig 2 | Macrolides and tetracyclines kill some human gut commensal species. **a**, The survival of 12 abundant human gut microbial species was measured after 5-h treatment with erythromycin, azithromycin or doxycycline at fivefold MIC concentrations (mean + s.d. of three independent experiments). CFUs per ml before treatment were set to 100%. Absolute values are indicated next to strain abbreviations: *Bf*, *B. fragilis*; *Bc*, *B. caccae*; *Bo*, *B. ovatus*; *Bt*, *B. thetaiotaomicron*; *Bu*, *B. uniformis*; *Bv*, *B. vulgatus*; *Cb*, *C. bolteae*; *Ec*, *E. coli* ED1a; *Er*, *E. rectale*; *Fn*, *F. nucelatum*; *Pc*, *P. copri*; *Ri*, *R. intestinalis*. Shaded area denotes bactericidal threshold; ND, not detected (detection limit: 1 CFU per ml); *, resistant strains. Species are plotted according to phylogeny. **b**, Erythromycin causes lysis in *B. vulgatus* and *B. uniformis*. Strains were grown for 3 h (arrow) before adding (orange) or not (black) 15 μg ml^{-1} erythromycin (fivefold MIC). Growth curves depict mean ± s.d. (dashed line) of three independent experiments. **c**, Erythromycin induces blebbing, cytoplasmic shrinkage and lysis (white arrows) in *B. vulgatus* and *B. uniformis*. Representative images of phase contrast videos (Supplementary Information) acquired after erythromycin treatment. Scale bar, 5 μm. **d**, The commensal *E. coli* ED1a is more susceptible to doxycycline killing than lab *E. coli* (BW25113), despite both strains having the same MIC (4 μg ml^{-1}). Survival of *E. coli* strains was measured in monocultures or as part of 12-member communities (all species from **a**) after 5-h treatment with fivefold MIC doxycycline (mean ± s.d. of 3–6 independent experiments). CFUs per ml before treatment were set to 100%. **e**, *E. coli* ED1a, but not BW25113, is eliminated from community after two rounds of doxycycline treatment. A 12-member community (as in **d**) containing either *E. coli* ED1a or BW25113 was treated with doxycycline for 5 h (fivefold *E. coli* MIC), washed with PBS, treated again with doxycycline and re-grown in mGAM. CFUs per ml were counted to assess community (dashed lines) and *E. coli* (solid lines) survival; the mean ± s.d. of three independent experiments is shown. AZI, azithromycin; DOX, doxycycline; ERY, erythromycin.

the commensal *E. coli* ED1a (Fig. 2a, Extended Data Fig. 5b). This was also true during aerobic growth (Extended Data Fig. 6h). Doxycycline killed this natural isolate more efficiently than the *E. coli* K-12 laboratory strain, BW25113, both alone and when part of a 12-member synthetic community (Fig. 2d). We wondered whether this strain-specific killing of *E. coli* by doxycycline would affect the retention of *E. coli* in a microbial community during longer antibiotic exposures. Indeed, *E. coli* ED1a was eliminated from the same synthetic community after two rounds of doxycycline treatment, whereas BW25113 was retained and recovered after treatment stopped (Fig. 2e). Altogether, this selective bactericidal activity of macrolides and tetracyclines could explain their strong effect on gut microbiota composition. Conceivably, microorganisms killed by the antibiotic are more likely to be inadvertently lost from the community, whereas ones inhibited can recover easier after treatment stops.

As drug interactions are often species specific[30], we reasoned that a second drug could selectively antagonize the effect of antibiotics on gut bacteria but not on pathogens, acting as an antidote. Therefore, we screened the same library of 1,197 pharmaceuticals (Prestwick Chemical Library) for compounds that antagonize erythromycin or doxycycline on the abundant gut microorganisms *B. vulgatus* and *B. uniformis* (Extended Data Fig. 7a). Of the 19 identified hits (Extended Data Fig. 7b, Supplementary Table 5), we tested 14 over broader concentration ranges. Ten combinations retained substantial antagonistic activity (Extended Data Figs. 7c, d, 8). The strongest antidotes were the anticoagulant drug dicumarol, the uricosuric agent benzbromarone and two non-steroidal anti-inflammatory drugs, tolfenamic acid and diflunisal. Although dicumarol and benzbromarone rescued *B. vulgatus* from erythromycin and diflunisal from doxycycline, tolfenamic acid protected *B. vulgatus* from both drugs. The antidotes also partially rescued *B. vulgatus* killing by both antibiotics (Extended Data Fig. 7e) and protected other phylogenetically related, abundant gut commensals from erythromycin and doxycycline (Extended Data Figs. 8, 9a). Notably, antidotes did not affect antibiotic efficacy against pathogens for which those antibiotics are prescribed (Extended Data Fig. 9b, Supplementary Table 1). Consistently, tolfenamic acid and dicumarol

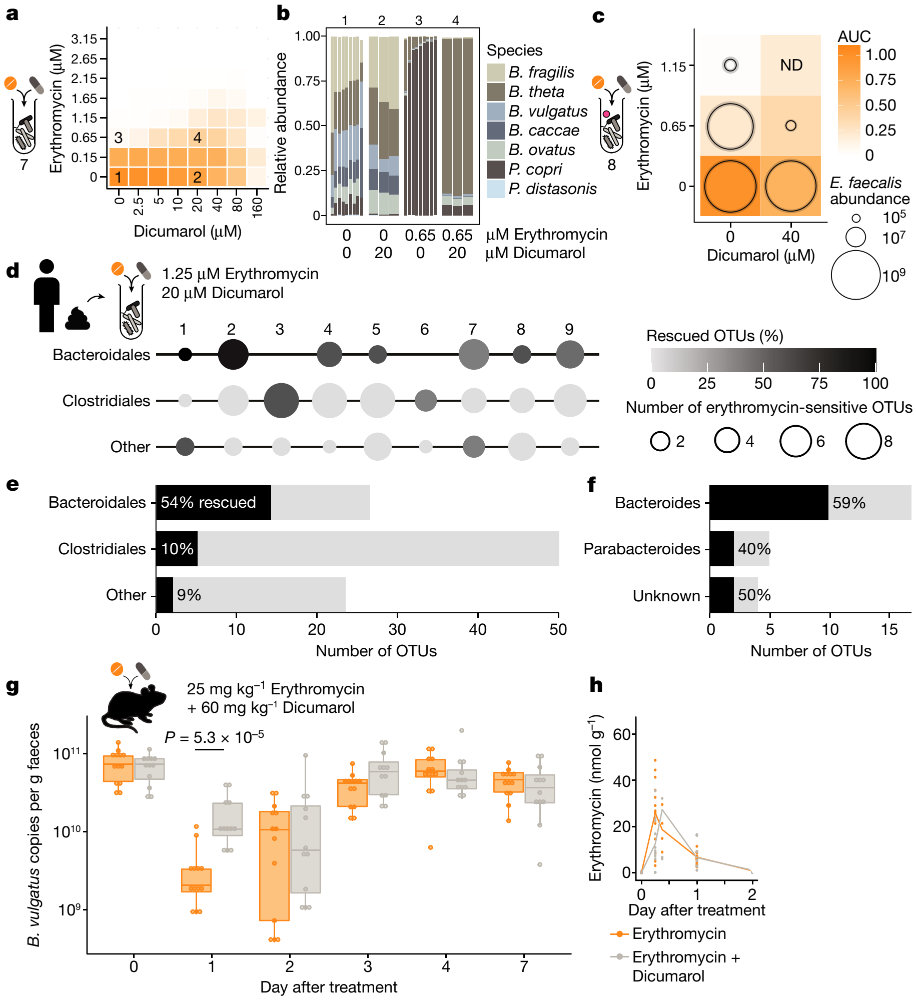

Fig 3 | Dicumarol selectively protects *Bacteroides* species from erythromycin in microbial communities. a, Checkerboard assay with a synthetic seven-member gut microbial community of Bacteroidales species (*B. caccae*, *B. fragilis* NT, *B. ovatus*, *B. thetaiotaomicron*, *B. vulgatus*, *P. copri* and *P. distasonis*) indicates that dicumarol rescues overall community growth. Heat map depicts median growth across triplicates. **b**, Community compositions in selected erythromycin–dicumarol concentration combinations (1–4 referring to checkerboard tiles in **a**) show that dicumarol alone does not alter community structure but rescues *Bacteroides* species from erythromycin (primarily *B. thetaiotaomicron* and *B. ovatus*, consistent with Extended Data Fig. 9a). Depicted are relative abundances of individual replicates as determined by 16S rRNA sequencing and rescaled to 100%. **c**, When the Bacteroidales community contains the pathogen *E. faecalis*, the antidote dicumarol rescues community growth upon erythromycin treatment but allows erythromycin to still target *E. faecalis* (even enhances its activity). Tiles show medians of normalized community growth, and circles within tiles represent the mean ± s.d. CFUs per ml of *E. faecalis* (3 biological × 2 technical replicates; initial inoculum: 1.25×10^6 CFUs per ml). ND, not detected (detection limit: 10^4 CFUs per ml). **d**–**f**, In complex human stool-derived communities from nine healthy donors, dicumarol protects most Bacteroidales OTUs from erythromycin (per order (**e**); per genus (**f**)) and at least one sensitive Bacteroidales OTU per individual. Circle diameter depicts the number of OTUs per order inhibited by erythromycin and gradient fill the fraction of these OTUs rescued by dicumarol (2 biological × 2 technical replicates). All Bacteroidales of donors 3 and 6 are resistant to the erythromycin concentrations used. **g**, Administration of dicumarol mitigates the decrease in faecal *B. vulgatus* counts that erythromycin causes in gnotobiotic mice colonized with a 12-member mouse microbiome[31] and *B. vulgatus*. The mice were treated once orally with either erythromycin ($n = 13$) or erythromycin–dicumarol ($n = 12$) in three independent experiments. Boxes are plotted as in Fig. 1c. Only *P* values for significant differences (two-sided Mann–Whitney *U*-test) between two groups of mice on the same day are shown. **h**, Faecal erythromycin concentrations and kinetics do not differ between the two groups of mice.

rescued the growth of most tested *Bacteroidetes* species at clinically relevant erythromycin concentrations but allowed erythromycin to act against relevant pathogens (Extended Data Figs. 9c, 11a).

We wondered whether antidotes would also work in community settings. All three antidotes that antagonized erythromycin also protected a synthetic microbial community composed of seven members of the order Bacteroidales (Fig. 3a, Extended Data Figs. 10a, 11b). The antidotes did not affect community structure when used alone but protected several *Bacteroides* species when combined with erythromycin and prevented the *Prevotella copri* dominance in the community upon erythromycin treatment (Fig. 3b, Extended Data Figs. 10b, 11c). When including the opportunistic pathogen *Enterococcus faecalis* in these communities, the antidote allowed erythromycin to eradicate *E. faecalis* from the community, but the community could now grow (Fig. 3c, Extended Data Fig. 10c). We then tested the antidote on nine different complex communities derived from human stool, and all antidotes preferentially rescued Bacteroidales operational taxonomic units (OTUs) from erythromycin (Fig. 3d–f, Extended Data Figs. 10d–f, 11d–f). Hence, the antidote effect holds largely true, independent of the Bacteroidales species and strains that each individual carries. Finally, we tested the ability of dicumarol and benzbromarone to act as macrolide antidote for *B. vulgatus* in vivo. First, we stably colonized gnotobiotic mice harbouring a defined 12-member mouse microbiome[31] with *B. vulgatus* and then applied a single oral erythromycin dose alone or together with the antidote. All animals showed significant decrease in *B. vulgatus* counts 1 d after erythromycin treatment. However, antidote co-treatment mitigated this temporal decline, especially for dicumarol (Fig. 3g, Extended Data Fig. 10g). This effect was not due to changes in faecal erythromycin levels, which were similar for single- and double-drug treatments, and peaked shortly after administration (Fig. 3h, Extended Data Fig. 10h).

Altogether, we provide a route for identifying antidotes that specifically mitigate the collateral damage of antibiotics on commensals, particularly on *Bacteroides* spp. This concept needs further development before any application—for example, antidotes should be tested for dosing or formulation to optimize pharmacokinetics and minimize adverse effects from their primary action. Currently, benzbromarone and dicumarol reach high enough colon concentrations when taken in normal doses[2]. Dietary compounds might also bear antidote potential.

In summary, this study provides a high-resolution map of the direct effect of antibiotics on human gut bacteria (Supplementary Table 1) down to the level of individual drugs, species and some selected strains. Because this study was not designed to establish translational relevance, future work will be needed to assess the generalisability of these findings, given the intraspecies variation among bacteria. Nevertheless, our results challenge the traditional view that antibiotics are bona fide bacteriostatic or bactericidal, as this hard division breaks in non-model bacteria. Antibiotics that preferentially kill some species might be most detrimental to the gut microbiota, although the first studies in limited numbers of healthy individuals point to the gut microbiota having some resilience against specific antibiotic regimens[32]. Understanding the underlying mechanisms for this selective killing might open up ways for the development of new antimicrobials and strategies for controlled microbiome modulation[33]. Overall, interactions of antibiotics and commensals merit deeper exploration, and we anticipate future studies on the variation of antibiotic susceptibility within individual gut microbiomes and its relation to drug use, as well as on the specific antibiotic mode(s) of action and resistance in gut commensals.

Online content

Any methods, additional references, Nature Research reporting summaries, source data, extended data, supplementary information, acknowledgements, peer review information; details of author contributions and competing interests; and statements of data and code availability are available at https://doi.org/10.1038/s41586-021-03986-2.

1. Blaser, M. J. Antibiotic use and its consequences for the normal microbiome. *Science* **352**, 544–545 (2016).
2. Maier, L. et al. Extensive impact of non-antibiotic drugs on human gut bacteria. *Nature* **555**, 623–628 (2018).
3. Cho, I. et al. Antibiotics in early life alter the murine colonic microbiome and adiposity. *Nature* **488**, 621–626 (2012).
4. Cox, L. M. et al. Altering the intestinal microbiota during a critical developmental window has lasting metabolic consequences. *Cell* **158**, 705–721 (2014).
5. Ruiz, V. E. et al. A single early-in-life macrolide course has lasting effects on murine microbial network topology and immunity. *Nat. Commun.* **8**, 518 (2017).
6. Korpela, K. et al. Intestinal microbiome is related to lifetime antibiotic use in Finnish pre-school children. *Nat. Commun.* **7**, 10410 (2016).
7. Parker, E. P. K. et al. Changes in the intestinal microbiota following the administration of azithromycin in a randomised placebo-controlled trial among infants in south India. *Sci. Rep.* **7**, 9168 (2017).
8. Falony, G. et al. Population-level analysis of gut microbiome variation. *Science* **352**, 560–564 (2016).
9. Rothschild, D. et al. Environment dominates over host genetics in shaping human gut microbiota. *Nature* **555**, 210–215 (2018).
10. Zimmermann, M., Patil, K. R., Typas, A. & Maier, L. Towards a mechanistic understanding of reciprocal drug–microbiome interactions. *Mol. Syst. Biol.* **17**, e10116 (2021).
11. Vich Vila, A. et al. Impact of commonly used drugs on the composition and metabolic function of the gut microbiota. *Nat. Commun.* **11**, 362 (2020).
12. Kuhn, M., Letunic, I., Jensen, L. J. & Bork, P. The SIDER database of drugs and side effects. *Nucleic Acids Res.* **44**, D1075–D1079 (2016).
13. Dethlefsen, L. & Relman, D. A. Incomplete recovery and individualized responses of the human distal gut microbiota to repeated antibiotic perturbation. *Proc. Natl Acad. Sci. USA* **108**, 4554–4561 (2011).
14. Uzan-Yulzari, A. et al. Neonatal antibiotic exposure impairs child growth during the first six years of life by perturbing intestinal microbial colonization. *Nat. Commun.* **12**, 443 (2021).
15. Nagy, E., Boyanova, L., Justesen, U. S. & ESCMID Study Group of Anaerobic Infections. How to isolate, identify and determine antimicrobial susceptibility of anaerobic bacteria in routine laboratories. *Clin. Microbiol. Infect.* **24**, 1139–1148 (2018).
16. European Committee on Antimicrobial Susceptibility Testing. Breakpoint tables for interpretation of MICs and zone diameters. v.; http://www.eucast.org/clinical_breakpoints/ (2019).
17. Bullman, S. et al. Analysis of *Fusobacterium* persistence and antibiotic response in colorectal cancer. *Science* **358**, 1443–1448 (2017).
18. Manfredo Vieira, S. et al. Translocation of a gut pathobiont drives autoimmunity in mice and humans. *Science* **359**, 1156–1161 (2018).
19. Gaulton, A. et al. The ChEMBL database in 2017. *Nucleic Acids Res.* **45**, D945–D954 (2017).
20. Slimings, C. & Riley, T. V. Antibiotics and hospital-acquired *Clostridium difficile* infection: update of systematic review and meta-analysis. *J. Antimicrob. Chemother.* **69**, 881–891 (2014).
21. Baron, S., Diene, S. & Rolain, J.-M. Human microbiomes and antibiotic resistance. *Hum. Microb. J.* **10**, 43–52 (2018).
22. Tramontano, M. et al. Nutritional preferences of human gut bacteria reveal their metabolic idiosyncrasies. *Nat. Microbiol.* **3**, 514–522 (2018).
23. Habib, G. et al. 2015 ESC Guidelines for the management of infective endocarditis: the Task Force for the Management of Infective Endocarditis of the European Society of Cardiology (ESC). Endorsed by: European Association for Cardio-Thoracic Surgery (EACTS), the European Association of Nuclear Medicine (EANM). *Eur. Heart J.* **36**, 3075–3128 (2015).
24. Kasper, D.L., F. A., Hauser S. L. & Longo D. L. *Harrison's Principles of Internal Medicine* (McGraw-Hill, 2012).
25. Lobritz, M. A. et al. Antibiotic efficacy is linked to bacterial cellular respiration. *Proc. Natl Acad. Sci. USA* **112**, 8173–8180 (2015).
26. French, G. L. Bactericidal agents in the treatment of MRSA infections—the potential role of daptomycin. *J. Antimicrob. Chemother.* **58**, 1107–111 (2006).
27. Jelic, D. & Antolovic, R. From erythromycin to azithromycin and new potential ribosome-binding antimicrobials. *Antibiotics (Basel)* **5**, 29 (2016).
28. Nemeth, J., Oesch, G. & Kuster, S. P. Bacteriostatic versus bactericidal antibiotics for patients with serious bacterial infections: systematic review and meta-analysis. *J. Antimicrob. Chemother.* **70**, 382–395 (2015).
29. Wald-Dickler, N., Holtom, P. & Spellberg, B. Busting the myth of "static vs cidal" a systemic literature review. *Clin. Infect. Dis.* **66**, 1470–1474 (2018).
30. Brochado, A. R. et al. Species-specific activity of antibacterial drug combinations. *Nature* **559**, 259–263 (2018).
31. Brugiroux, S. et al. Genome-guided design of a defined mouse microbiota that confers colonization resistance against *Salmonella enterica* serovar Typhimurium. *Nat. Microbiol.* **2**, 16215 (2016).
32. Palleja, A. et al. Recovery of gut microbiota of healthy adults following antibiotic exposure. *Nat. Microbiol.* **3**, 1255–1265 (2018).
33. Schmidt, T. S. B., Raes, J. & Bork, P. The human gut microbiome: from association to modulation. *Cell* **172**, 1198–1215 (2018).

Methods

Growth conditions

Species names in this manuscript refer to the strains listed in Supplementary Table 1 and are only further specified if different strains of the same species were tested. All experiments from this study were performed in an anaerobic chamber (Coy Laboratory Products) (2% H_2, 12% CO_2, 86% N_2), and all materials and solutions used for these experiments were pre-reduced for at least 24 h before use, unless specified otherwise. Bacteria used in this study were typically pre-cultured for two overnights. Cells were cultured in 5 ml of modified Gifu anaerobic medium (mGAM) broth (HyServe, produced by Nissui Pharmaceuticals) and grown at 37 °C overnight. The next day, cells were diluted 1/100 in 5 ml of mGAM medium and grown at 37 °C overnight before starting the experiments.

Quantitative assay for MIC determination with MIC test strips

MIC test strips were purchased from Liofilchem or Oxoid (Supplementary Table 3). All MICs were measured under anaerobic growth conditions inside a Coy anaerobic chamber. Bacteria were pre-cultured in mGAM for two nights, and cultures were diluted to $OD_{578} = 0.5$. Next, 50 µl of the diluted culture was spread on an mGAM agar plate and allowed to dry for 15 min. The MIC test strip was placed on the agar with sterile tweezers, allowing the part with the lowest concentration to touch the agar first. Plates were incubated at 37 °C inside the anaerobic chamber overnight and for longer depending on the species-specific growth requirements. After formation of a symmetrical inhibition ellipse, plates were taken out of the chamber and imaged under controlled lighting conditions (spImager, S&P Robotics) using an 18-megapixel Canon Rebel T3i camera. MICs were directly determined from the strip scale at the point where the edge of the inhibition ellipse intersects the MIC test strip. All MICs were determined in duplicates. In cases of an eightfold difference between the two values, a third replicate was done. In all cases, this resulted in a clear outlier (more than eightfold different from other two MICs) that was removed from the dataset.

MIC comparison to ChEMBL and EUCAST databases

Previously known MICs were extracted from the ChEMBL database (version 24)[19] and EUCAST (obtained on 14 May 2018)[16]. Antibiotics from these two datasets were mapped to our dataset by compound name. Species were mapped using NCBI taxonomy identifiers and species names. For MICs from ChEMBL, a keyword-based approach was used to exclude experiments on species with modifications such as mutations, deletions and insertions. The EUCAST database contains a large number of reported MICs for each compound–species pair. We collapsed these to a single value by calculating the median MIC.

Estimates on the abundance and prevalence of species in the healthy human gut microbiome were calculated using mOTUs version 2 (ref. [34]) as follows. Relative species abundances were determined in 727 shotgun metagenomic samples from donors in the control groups of multiple studies from various countries and continents[35–39]. Before taxonomic profiling, metagenomes were quality controlled using the MOCAT2 -rtf procedure[40], which removed reads with at least 95% sequence identity and an alignment length of at least 45 bp to the human genome hg19. Taxonomic profiles were then created using mOTUs version 2.1.0 (ref. [34]) with parameters -l 75; -g 2; and -c. Afterwards, relative abundances below 10^{-4} were set to zero, and species with non-zero abundance in fewer than five samples were discarded. For the retained 1,350 species, prevalence was defined as the percentage of samples with non-zero abundance; a prevalence cutoff of 1% was chosen to classify species into 'rare' and 'common' species. For all species in the MIC dataset, we manually assessed their status as pathogenic or non-pathogenic species using literature . Pathogenic species that occur in more than 1% of healthy people (that is, are designated as common') were classified as 'potentially pathogenic species' that can, for example, cause diseases in immunocompromised patients.

Killing curves and survival assay

Cells were pre-cultured as described in the 'Growth conditions' section before being diluted to an $OD_{578} = 0.01$ and grown for 2 h at 37 °C (unless specified otherwise). Next, cells were diluted 1/2 in mGAM containing a tenfold MIC of erythromycin, azithromycin or doxycycline (final antibiotic concentration is fivefold MIC) and incubated in the presence of the antibiotic for 5 h at 37 °C. Fivefold antibiotic MICs are conventionally used in killing curves to be well above the MIC value. As MICs are not fully precise values and can slightly vary from one experimental setup to the other, using 5× MIC ensures that a concentration is reached that is effective in preventing bacterial growth. At several time points (0 h, 1 h, 2 h, 3 h, 4 h and 5 h), 100 µl of cells were serial diluted in PBS (10^{-1} to 10^{-8} dilutions) and plated on mGAM-agar plates for CFU counting. When no cells were detected using this method, a greater volume of culture (up to 2 ml) was plated to be able to detect CFUs. Agar plates were incubated overnight at 37 °C, and colonies were counted the next day, either manually, for low CFU numbers, or using the Analyze Particles tool from ImageJ[41]. Data were plotted with GraphPad Prism, version 8.

Live/dead staining

Cells were pre-cultured as described in the 'Growth conditions' section before being diluted to an $OD_{578} = 0.01$ and grown for 2 h at 37 °C. Cells were next diluted 1/2 in mGAM containing tenfold MIC of erythromycin, azithromycin or doxycycline (final concentration is fivefold the MIC) and incubated in the presence of the antibiotic for 5 h at 37 °C. Then, cells were live/dead stained using the LIVE/DEAD BacLight Bacterial Viability and Counting Kit (no. L34856, Molecular Probes, Thermo Fisher Scientific) according to the manufacturer's protocol, before and after antibiotic treatment.

Flow cytometry

Stained cells were counted using a BD LSRFortessa flow cytometer (BD FACSDiva software, version 8.0.2). The forward (FSC) and side scatter (SSC) signals (488 nm) as well as the green and red fluorescent signals (488–530/30A filter and 561–610/20A filter, respectively) were acquired. The FSC/SSC detectors were set to logarithmic scale, and gates were set as illustrated in Supplementary Fig. 1. The flow rate varied between 12 µl min^{-1} and 60 µl min^{-1} depending on the concentration of each sample, and the analysis was stopped when 10,000 target events were measured. Graphs were generated using FlowJo version 10.3 software (TreeStar).

Microscopy

For live/dead imaging, stained cells were washed twice in 0.85% NaCl before being spotted on 0.85% NaCl + 1% agarose pads between a glass slide and a coverslip. For time-lapse imaging, cells were pre-cultured as described in the 'Growth conditions' section. Cells were then diluted to an $OD_{578} = 0.01$ and grown for 3 h at 37 °C before being spotted on mGAM + 1% agarose pads and supplemented or not with 15 µg ml^{-1} of erythromycin (fivefold MIC) between a glass slide and a coverslip. Slides were sealed with valap (to avoid or at least, delay oxygen permeation) and taken outside the anaerobic chamber for imaging. In these conditions, untreated bacteria kept growing rapidly (Videos 1, 3). The imaging was performed using a Nikon Eclipse Ti inverted microscope, equipped with a Nikon DS-Qi2 camera, a Nikon Plan Apo Lambda ×60 oil Ph3 DM phase-contrast objective and a Nikon HC mCherry filter set (Ex 562/40; DM 593; BA 641/75) to detect propidium iodide fluorescence. Images were acquired with NIS-Elements AR4.50.00 software and processed with Fiji v.2.0.0-rc-68/1.52h[42].

Growth curves

Cells were pre-cultured as described in the 'Growth conditions' section. Then, cells were diluted to an $OD_{578} = 0.01$ in a 96-well plate sealed with a breathable membrane (Breathe-Easy, Sigma-Aldrich) and grown for 2 h.

Next, erythromycin was added to the culture to a final concentration of 15 μg ml^{-1} (fivefold MIC), and growth curves were acquired for 20 h using a microplate spectrophotometer (EON, Biotek, Gen5 software, version 3.05) by measuring the OD_{578} every hour after 30 s of linear shaking.

Community assembly

Monocultures were pre-cultured as described in the 'Growth conditions' section. In the morning, communities were assembled by mixing equal amounts (volume depending on their individual OD) of the different species to reach a total OD of 0.01 in mGAM. The 12-member community (Fig. 2) was assembled from monocultures of *B. fragilis*, *B. uniformis*, *B. thetaiotaomicron*, *B. ovatus*, *B. caccae*, *B. vulgatus*, *P. copri*, *Fusobacterium nucleatum*, *Clostridium boltae*, *Eubacterium rectale*, *Roseburia intestinalis* and *E. coli* ED1a or BW25113 (Supplementary Table 1).

To test for *E. coli* survival, the communities were subsequently grown for 2 h and treated with doxycycline (20 μg ml^{-1}; fivefold MIC) for 5 h. Then, 100 μl of cells was serial diluted in PBS (10^{-1} to 10^{-8} dilutions) in the absence of oxygen and plated on mGAM-agar plates for CFU counting of the whole community. To specifically count *E. coli* survivors, the same dilutions were plated on LB-agar plates in the presence of oxygen, as none of the other community members grew under aerobic conditions. Plates were incubated at 37 °C overnight, and colonies were counted the next day, either manually, for low CFU numbers, or using the Analyze Particles tool from ImageJ[41].

To test the fate of *E. coli* strains as part of a synthetic community, cells were grown, assembled in a community as described above and treated with doxycycline (20 μg ml^{-1}; fivefold MIC). After the first 5-h treatment, communities were centrifuged, washed with PBS three times to remove residual doxycycline and kept in PBS overnight. The next day, communities were re-suspended in mGAM containing doxycycline (20 μg ml^{-1}; fivefold MIC) and incubated at 37 °C for 5 h. They were then washed again with PBS three times and re-suspended in mGAM without drug for recovery. CFUs per ml of *E. coli* were counted in all cases.

Screen for microbiome-protective antibiotic antagonism

Preparation of screening plates. The Prestwick Chemical Library was purchased from Prestwick Chemical, and drugs were re-arrayed, diluted and stored in 96-well format as described previously[2]. We prepared drug plates (2× drug concentration) in mGAM medium and stored them at −30 °C. For each experiment, drug plates were thawed, supplemented with the respective antibiotic solution (freshly prepared in mGAM) and pre-reduced in the anaerobic chamber overnight. All rearranging and aliquoting steps were done using the Biomek FXP (Beckman Coulter) system.

Inoculation and screening conditions. Strains were grown twice overnight; the second overnight culture was diluted in mGAM to reach $OD_{578} = 0.04$ (4× the desired starting OD). Next, 25 μl of the diluted cultures was used to inoculate wells containing 50 μl of 2× concentrated Prestwick drug and 25 μl of the 4× concentrated antibiotic using the semi-automated, 96-well multi-channel pipette epMotion 96 (Eppendorf). Each well contained 1% DMSO, 20 μM of the Prestwick drug and a species-specific antibiotic concentration that was just inhibitory for the respective strain (0.625 μM for erythromycin, 0.04 μM doxycycline for *B. uniformis* and 0.08 μM doxycycline for *B. vulgatus*). Plates were sealed with breathable membranes (Breathe-Easy), and OD_{578} was measured hourly after 30 s of linear shaking with a microplate spectrophotometer (Eon, BioTek, Gen5 software, version 3.05) and an automated microplate stacker (BioStack 4, BioTek) fitted inside a custom-made incubator (EMBL Mechanical Workshop). Growth curves were collected up to 24 h. For each antibiotic, each species was screened in biological duplicates. All experiments included control wells of unperturbed growth (32 wells per run) and control wells for growth in the presence of the antibiotic only (eight wells per plate).

Analysis pipeline and hit calling. All growth curves within a plate were truncated at the transition time from exponential to stationary phase and converted to normalized areas under the curve (AUCs) using in-run control wells (no drug), as described previously[2]. We then calculated *z*-scores based on these normalized AUCs, removed replicates with eightfold differences in *z*-scores to eliminate noise effects, computed mean *z*-scores across the two replicates and selected combinations with mean *z*-scores greater than 3. This selection included 19 potential antibiotic antagonists, and we followed up on 14 of them (seven potential erythromycin and seven potential doxycycline antagonists in either *B. vulgatus* or *B. uniformis*; Extended Data Fig. 8) in independent experiments.

Validation of microbiome-protective antagonists. First, we kept the erythromycin–doxycycline concentration constant (0.625 μM for erythromycin and 0.078 μM (*B. vulgatus*)/0.039 μM (*B. uniformis*) for doxycycline) and tested concentration gradients of the potential antagonists with ranges depending on the solubility of the antagonist. Compounds were purchased from independent vendors (Supplementary Table 6) and dissolved at 100× starting concentration in DMSO. Eight twofold serial dilutions were prepared in 96-well plates, with each row containing a different antagonist, sufficient control DMSO wells and wells with just the respective antibiotic ('antibiotic-only' control). These master plates were diluted in mGAM medium (50 μl) to 2× assay concentration, and 25 μl of freshly prepared antibiotic solution (4× test concentration) was added. Plates were pre-reduced overnight in an anaerobic chamber and inoculated with 25 μl of overnight cultures (prepared as described in the 'Growth conditions' section) to reach a starting OD_{578} of 0.01 and 1% DMSO concentration. Growth was monitored hourly for 24 h after 30 s of linear shaking (as described for the screen[2]). Experiments were performed in biological triplicates. For analysis, growth curves were converted into normalized AUCs (see above). We accounted for residual growth in the presence of the antibiotic by subtracting the median normalized AUCs of the 'antibiotic-only' control per plate. We computed medians across triplicates and considered a normalized AUC greater than 0.25 as a concentration-dependent growth rescue by the antagonist.

Checkerboard assays for anaerobic commensals and pathogens. Validated antagonists were further investigated in 8 × 8 checkerboard assays, where both antibiotics and antagonists were titrated against each other. Such assays were first performed for the commensals that were originally screened (that is, *B. vulgatus* and *B. uniformis*—four replicates) and later expanded to six other gut microorganisms (*B. caccae*, *B. fragilis* NT, *B. ovatus*, *B. thetaiotaomicron*, *P. copri* and *Parabacteroides distasonis*—two replicates) and two pathogens (*E. faecalis* and *Enterococcus faecium*; Supplementary Table 1). For horizontal gradients, twofold serial dilutions of the antagonists were prepared first in 100× DMSO and diluted in mGAM as described above ('Validation of microbiome-protective antagonists' section). Vertical antibiotic dilution series were freshly prepared in mGAM at 4× final concentration in twofold serial dilution steps. Both vertical and horizontal dilution series were combined (50 μl of the antagonist gradients (2×) and 25 μl of the antibiotic gradients (4×)) in 96-well plates. Plates were pre-reduced under anaerobic conditions overnight, inoculated with 25 μl of diluted overnight culture (at 4× starting OD) and sealed with a breathable membrane (Breathe-Easy). Bacterial growth was monitored once per hour for 24 h after 60 s linear shaking (Eon + BioStack 4, BioTek) under anaerobic conditions. Growth curves were converted into normalized AUCs as described using in-plate controls to define unperturbed growth.

Checkerboard assays for pathogens under aerobic conditions. For *Staphylococcus aureus* DSM 20231, 8 × 8 checkerboard assays were performed under aerobic conditions in tryptic soy broth using 384-well plates (Greiner Bio-One), with each well containing a total volume of 50 µl. Antidotes were arrayed in the checkerboards in twofold serial dilutions, whereas antibiotics were diluted over a more resolved, evenly spaced gradient, starting from the highest concentration selected. Cells were inoculated at initial OD_{595} ~0.01 from an overnight culture. Plates were sealed with breathable membranes (Breathe-Easy) and incubated at 37 °C with continuous shaking. OD_{595} was measured every 30 min for 16 h. Background due to medium was subtracted, and growth curves were trimmed at the transition to stationary phase (6.5 h for *S. aureus*). AUCs were calculated and normalized by the median of the no-drug control wells present in each plate ($n = 6$). All experiments were done in at least three biological replicates.

Antidote testing in synthetic microbial communities

Checkerboard assays for synthetic microbial communities. The seven-member community was composed of *B. vulgatus*, *B. fragilis* NT, *B. thetaiotaomicron*, *P. copri*, *B. ovatus*, *B. caccae* and *P. distasonis* and was supplemented with *E. faecalis* when indicated. Monocultures were diluted to OD_{578} (4× desired starting OD) with equal contribution of each member. Checkerboard assays were conducted in mGAM as described for monocultures. For enumeration of final *Enterococci* counts within synthetic communities, appropriate dilutions of communities were plated out on *Enterococci* selective medium (azide dextrose broth-based, Oxoid, CM0868) and grown under aerobic conditions. To determine the community composition for selected antidote–antibiotic concentration combinations, the reaction mixture was scaled up to 1-ml volume, and the cell pellet was collected after 24-h incubation.

DNA extraction and 16S sequencing from synthetic and human-stool-derived communities. DNA was extracted in 96 deep-well plates. Cells were first washed with PBS and re-suspended in 281 µl of cell suspension solution (MP GNOME DNA kit). Cell suspension was treated with lysozyme (25 µl; 400,000 U ml^{-1}) and incubated for 1 h at 37 °C. Cell suspensions were then further lysed by three freeze–thaw cycles using liquid nitrogen, before the addition of 15.2 µl of cell lysis solution (MP GNOME DNA kit) and 20 µl of RNA mix (MP GNOME DNA kit). A last step of lysis was performed using glass beads (Glasperlen, Edmund Bühler) by bead beating twice for 5 min at 30 Hz in a Tissue Lyzer II (Qiagen) and by three freeze–thaw cycles in liquid nitrogen. Lysates were then incubated for 30 min at 37 °C with shaking. Next, 12.8 µl of protease mix (MP GNOME DNA kit) was added, and the lysates were incubated for 2 h at 55 °C. After a 5-min centrifugation step at 3,200*g*, 200 µl of supernatant was collected and mixed with 100 µl of TENP buffer[43] (50 mM Tris-HCl, pH 8, 20 mM EDTA, 100 mM NaCl, 1% w/v polyvinylpolypyrrolidone). These supernatants were then incubated for 10 min with 75 µl salt out solution (MP GNOME DNA kit) at 4 °C. After a 10-min centrifugation at 3,200*g*, 200 µl of supernatant was transferred to a clean plate. Then, 500 µl of ice-cold ethanol and 70 µl of 3 M NaOAc pH 5.2 were added. The solution was kept at −30 °C overnight. The next day, plates were centrifuged at 4 °C at 3,200*g* for 45 min. The supernatant was carefully removed, and the pellets were washed with 400 µl of ice-cold 70% ethanol. After 20-min centrifugation at 3,200*g* at 4 °C, all the supernatant was removed, and plates were dried in a chemical hood. DNA was re-suspended in 70 µl of water overnight at 4 °C. The 16S libraries were then prepared for sequencing using a two-step polymerase chain reaction (PCR) method according to ref. [44], using the Phire Hot Start II DNA Polymerase (Thermo Fisher Scientific). In brief, the V4 region was amplified by a first PCR. These amplicons were subsequently amplified again using barcoded primers that contain Illumina adaptors. These libraries were sequenced on a MiSeq (250 PE).

16S rRNA amplicon data processing and analysis for synthetic communities. Raw reads were quality trimmed, de-noised and filtered against chimeric PCR artefacts using DADA2 version 1.18.0 (ref. [45]). Resulting amplicon sequence variants (ASVs) were mapped against the full-length 16S rRNA gene sequences of expected species using BLAST[46] to determine species relative abundances through total sum scaling. ASVs mapping with less than 98% (maximum two mismatches) to any of the expected species were treated as contamination but attracted a negligible number of reads overall. Triplicates were summarized via the median of species relative abundances and re-scaled to 100%.

Antidote testing in human-stool-derived communities

The EMBL Bioethics Internal Advisory Committee approved all experiments involving human stool-derived material, and informed consent was obtained from all donors (BIAC2015-009). Fresh stool samples from nine healthy volunteers were immediately placed in an anaerobic chamber, mixed 1:1 (wt/vol) with 40% glycerol in PBS + 0.5 g L^{-1} cysteine, stirred and aliquoted into 700-µl glycerol stocks. For each of the donors, one aliquot was diluted in 50 ml of mGAM medium, serially diluted and grown at 37 °C under anaerobic conditions for 24 h. After the 24-h incubation, 800 µl of the serially diluted cultures was mixed with 200 µl of 50% glycerol and stored at −80 °C for a maximum of 7 months. For antidote assays, microbial communities derived from the 1,000-fold dilution frozen stock were inoculated into fresh mGAM overnight. Each community was diluted to reach the starting OD_{578} of 0.01 in deep-well plates containing the indicated antibiotic–antidote combinations in fresh mGAM medium (final volume was 1 ml per well). Deep-well plates were incubated at 37 °C for 20 h under anaerobic conditions, and cell pellets were harvested by centrifugation. DNA extraction and 16S sequencing were performed as described above. Assays were performed in two biological replicates with two technical replicates each.

16S rRNA amplicon data processing from stool-derived communities. Raw reads were quality trimmed, de-noised and filtered against chimeric PCR artefacts using DADA2 version 1.8.0 (ref. [45]). The resulting exact ASVs were taxonomically classified and mapped to a reference set of OTUs at 98% sequence similarity using MAPseq version 1.2.3 (ref. [47]). Reads that did not confidently map to the reference were aligned to bacterial and archaeal secondary structure-aware small ribosomal subunit rRNA models using Infernal version 1.1.2 (ref. [48]) and clustered into OTUs with 98% average linkage using HPC-CLUST version 1.2.1 (ref. [49]), as described previously[50]. Sequencing experiments, which yielded fewer than 2,000 reads, and OTUs with fewer than ten reads across all conditions were discarded. Combined fold changes and *P* values were computed from all replicates using DESeq2 version 1.32.0 (refs. [51,52]) without filtering outliers. We corrected for multiple hypothesis testing[53] separately for each of the three antidotes. OTUs inhibited by erythromycin compared to untreated samples were first determined (adjusted $P < 0.1$, more than twofold reduction). For these OTUs, we computed adjusted *P* values for the abundance change between treatments with erythromycin alone and with both erythromycin and the antidote under consideration. An OTU was considered to be rescued by the antidote if the adjusted *P* value was below 0.1 and there was at least a twofold increase.

Antidote testing in a gnotobiotic animal model

Animal experiments. All animal experiments were approved by the local authorities (Regierung von Oberbayern, ROB-55.2-2532.Vet_02-17-120). Gnotobiotic C57BL/6J mice that were stably colonized with the Oligo-Mouse-Microbiota bacterial consortium[31]—housed at 22 ± 1.5 °C, 50 ± 5% humidity, 12-hour light/dark cycle and bred in flexible film isolators (North Kent Plastic)—were used in this study. For all experiments, female and male mice between 6 and 12 weeks old were used, and animals were randomly assigned to experimental groups. During experiments, gnotobiotic mice were supplied with autoclaved ddH_2O and Mouse-Breeding complete feed for mice (ssniff) ad libitum. All animals were scored twice daily for health status. Mice were pre-colonized with *B. vulgatus* DSM 1447 by administration of a *B. vulgatus* culture, 50 µl orally and 100 µl rectally, 7–10 d before drug treatment. Mice were treated by oral gavage with a single dose of 25 mg kg^{-1} erythromycin, a combination of 25 mg kg^{-1} erythromycin plus 60 mg kg^{-1} dicumarol[54] or a combination of 25 mg kg^{-1} erythromycin plus 50 mg kg^{-1} benzbromarone[55]. All drugs or drug combinations were applied as suspension in 100 µl of sterile corn oil. Two faecal pellets per mouse were collected before drug treatment and at 6 h, 9 h, day 1, day 2, day 3, day 4 and day 7 after treatment. One pellet was used for the enumeration of *B. vulgatus* counts; the second pellet was used to determine the faecal antibiotic concentration. At day 7 after treatment, mice were killed by cervical dislocation.

DNA extraction from faecal samples and enumeration of faecal *B.vulgatus* copy numbers. For gDNA extraction from faecal pellets, the phenol–chloroform method as described in ref. [56] was used. To quantify *B. vulgatus* copy numbers, quantitative PCR was performed as previously described[31] using *B. vulgatus* 16S rRNA-specific primers (NT5001_fwd1: TGGATGCCAATCCCCAAA, NT5001_rev1: GTGGAGTCGGGTTGCAGACT, NT5001_probe1: CCTCTCTCAGTTCGGACTG with 5′ HEX - 3′ BHQ-1 modifications). qPCR standard curves were determined using linearized plasmid as DNA template.

Quantification of faecal drug concentrations

Chemicals and equipment. All chemicals for liquid chromatography–mass spectrometry (LC–MS) analysis, including water and acetonitrile (LC–MS grade), were purchased from Thermo Fisher Scientific. Standards for online mass calibration were purchased from Agilent Technologies.

Sample preparation. Next, 300 µl of solvent mixture (acetonitrile:methanol, 1:1) containing the internal standard warfarin at 640 nM and one tungsten carbide bead (3 mm) from Qiagen were added to each faecal sample. Samples were homogenized by bead-beating on a Qiagen TissueLyser II at 30 Hz for 5 min. The lysed samples were centrifuged at 10,000 relative centrifugal force at 4 °C for 12 min. Equal volumes (70 µl) of extraction supernatant and water were mixed in Nunc 96-well, V-shape plates. Finally, 10-µl samples were further diluted in 30 µl of water for LC–MS analysis.

LC–MS measurements. Chromatographic separation was performed using an Agilent InfinityLab Poroshell 120 HPHC-C18, 3.0 mm × 150 mm, 1.9-µm column and an Agilent 1290 Infinity II LC system coupled to a 6550 iFunnel qToF mass spectrometer. The column temperature was maintained at 45 °C with a flowrate of 0.5 ml min^{-1}. The following mobile phases were used: mobile phase A: water with 0.1% formic acid; mobile phase B: acetonitrile with 0.1% formic acid. Next, 5 µl of sample was injected at 5% mobile phase B, maintained for 0.10 min, followed by a linear gradient to 95% B for 10 min and maintained at 95% B for 1 min. The column was allowed to re-equilibrate with starting conditions for 1.1 min before each sample injection. The mass spectrometer was operated in positive scanning mode (50–1,700 *m*/*z*) in positive scanning mode (50–1,700 *m*/*z*) with previously reported parameters[57].

Standard curves for each compound were obtained by serially diluting each compound in water at twofold from 5 µM to 4.9 nM, and limits of detection for each compound were determined based on the resulting standard curves.

Quantification and data analysis. The MassHunter Qualitative Analysis Software (Agilent Technologies, version 10.0) was used to determine retention time for each compound. Peak integration was carried out using MassHunter Quantitative Analysis Software with the following setting: mass tolerance = 20 ppm, peak filter at signal-to-noise ratio = 3 and retention time tolerance of 0.2–0.5 min. Total drug amounts in each intestinal compartment were calculated using the corresponding total sample weight.

Phylogenetic analysis and phylogenetic tree construction

To generate a phylogenetic tree for the different isolates, the nucleotide sequences for a set of universally occurring, protein-coding, single-copy phylogenetic marker genes[34,58] were extracted from reference genomes or genome assemblies using fetchMG version 1.0 (ref. [58]) (https://motu-tool.org/fetchMG.html). Within the framework of the ete3 toolkit version 3.1.1 (ref. [59]), ClustalOmega version 1.2.4 (ref. [60]) was used to create sequence alignments for each marker gene independently, and all columns with more than 10% gaps were removed. The individual alignments were concatenated, and, finally, a phylogenetic tree was inferred from the combined alignment using IQTree version 1.5.5 (ref. [61]). In Fig. 2a, the tree is not shown due to space restrictions, but species are presented according to the tree order.

Reporting summary

Further information on research design is available in the Nature Research Reporting Summary linked to this paper.

Data availability

All primary data generated in this study are in the Article and its Supplementary Information and are available from Zenodo: (https://doi.org/10.5281/zenodo.3527540). Clinical breakpoints (Fig. 1c) were retrieved from the EUCAST database: https://eucast.org/clinical_breakpoints/. Source data are provided with this paper.

Code availability

Code for analysing data and generating the figures (except Fig. 2 and Extended Data Figs. 5, 6) is available at https://git.embl.de/maier/abxbug.

34. Milanese, A. et al. Microbial abundance, activity and population genomic profiling with mOTUs2. *Nat. Commun.* **10**, 1014 (2019).
35. Feng, Q. et al. Gut microbiome development along the colorectal adenoma-carcinoma sequence. *Nat. Commun.* **6**, 6528 (2015).
36. Vogtmann, E. et al. Colorectal cancer and the human gut microbiome: reproducibility with whole-genome shotgun sequencing. *PLoS ONE* **11** (2016).
37. Wirbel, J. et al. Meta-analysis of fecal metagenomes reveals global microbial signatures that are specific for colorectal cancer. *Nat. Med.* **25**, 679–689 (2019).
38. Yu, J. et al. Metagenomic analysis of faecal microbiome as a tool towards targeted non-invasive biomarkers for colorectal cancer. *Gut* **66**, 70–78 (2017).
39. Zeller, G. et al. Potential of fecal microbiota for early-stage detection of colorectal cancer. *Mol. Syst. Biol.* **10**, 766 (2014).
40. Kultima, J. R. et al. MOCAT2: a metagenomic assembly, annotation and profiling framework. *Bioinformatics* **32**, 2520–2523 (2016).
41. Schneider, C. A., Rasband, W. S. & Eliceiri, K. W. NIH Image to ImageJ: 25 years of image analysis. *Nat. Methods* **9**, 671–675 (2012).
42. Schindelin, J. et al. Fiji: an open-source platform for biological-image analysis. *Nat. Methods* **9**, 676–682 (2012).
43. Frostegård, A. et al. Quantification of bias related to the extraction of DNA directly from soils. *Appl. Environ. Microbiol.* **65**, 5409–5420 (1999).
44. Caporaso, J. G. et al. Global patterns of 16S rRNA diversity at a depth of millions of sequences per sample. *Proc. Natl Acad. Sci. USA* **108**, 4516–4522 (2011).
45. Callahan, B. J. et al. DADA2: high-resolution sample inference from Illumina amplicon data. *Nat. Methods* **13**, 581–583 (2016).
46. Altschul, S. F., Gish, W., Miller, W., Myers, E. W. & Lipman, D. J. Basic local alignment search tool. *J. Mol. Biol.* **215**, 403–410 (1990).
47. Matias Rodrigues, J. F., Schmidt, T. S. B., Tackmann, J. & von Mering, C. MAPseq: highly efficient k-mer search with confidence estimates, for rRNA sequence analysis. *Bioinformatics* **33**, 3808–3810 (2017).
48. Nawrocki, E. P. & Eddy, S. R. Infernal 1.1: 100-fold faster RNA homology searches. *Bioinformatics* **29**, 2933–2935 (2013).
49. Matias Rodrigues, J. F. & von Mering, C. HPC-CLUST: distributed hierarchical clustering for large sets of nucleotide sequences. *Bioinformatics* **30**, 287–288 (2014).
50. Schmidt, T. S. B., Matias Rodrigues, J. F. & von Mering, C. Limits to robustness and reproducibility in the demarcation of operational taxonomic units. *Environ. Microbiol.* **17**, 1689–1706 (2015).
51. Love, M. I., Huber, W. & Anders, S. Moderated estimation of fold change and dispersion for RNA-seq data with DESeq2. *Genome Biol.* **15**, 550 (2014).
52. McMurdie, P. J. & Holmes, S. Waste not, want not: why rarefying microbiome data is inadmissible. *PLoS Comput. Biol.* **10**, e1003531 (2014).
53. Benjamini, Y. & Hochberg, Y. Controlling the false discovery rate: a practical and powerful approach to multiple testing. *J. R. Stat. Soc. B* **57**, 289–300 (1995).
54. Chen, M. et al. Inhibition of renal NQO1 activity by dicoumarol suppresses nitroreduction of aristolochic acid I and attenuates its nephrotoxicity. *Toxicol. Sci.* **122**, 288–296 (2011).

55. Cai, H. Y. et al. Benzbromarone, an old uricosuric drug, inhibits human fatty acid binding protein 4 in vitro and lowers the blood glucose level in db/db mice. *Acta Pharmacol. Sin.* **34**, 1397–1402 (2013).
56. Herp, S. et al. *Mucispirillum schaedleri* antagonizes *Salmonella* virulence to protect mice against colitis. *Cell Host Microbe* **25**, 681–694 (2019).
57. Zimmermann, M., Zimmermann-Kogadeeva, M., Wegmann, R. & Goodman, A. L. Mapping human microbiome drug metabolism by gut bacteria and their genes. *Nature* **570**, 462–467 (2019).
58. Sunagawa, S. et al. Metagenomic species profiling using universal phylogenetic marker genes. *Nat. Methods* **10**, 1196–1199 (2013).
59. Huerta-Cepas, J., Serra, F. & Bork, P. ETE 3: reconstruction, analysis, and visualization of phylogenomic data. *Mol. Biol. Evol.* **33**, 1635–1638 (2016).
60. Sievers, F. et al. Fast, scalable generation of high-quality protein multiple sequence alignments using Clustal Omega. *Mol. Syst. Biol.* **7**, 539 (2011).
61. Nguyen, L. T., Schmidt, H. A., von Haeseler, A. & Minh, B. Q. IQ-TREE: a fast and effective stochastic algorithm for estimating maximum-likelihood phylogenies. *Mol. Biol. Evol.* **32**, 268–274 (2015).
62. Cani, P. D. & de Vos, W. M. Next-generation beneficial microbes: the case of *Akkermansia muciniphila*. *Front. Microbiol.* **8**, 1765 (2017).
63. Routy, B. et al. Gut microbiome influences efficacy of PD-1-based immunotherapy against epithelial tumors. *Science* **359**, 91–97 (2018).

Acknowledgements We thank S. Göttig and members of the Typas lab for feedback on the manuscript; A. R. Brochado for help with experimental design; and EMBL GeneCore and Flow Cytometry Core Facilities for services and experimental advice. We acknowledge EMBL, JPIAMR grant combinatorials and ERC grant uCARE (ID 819454) for funding. L.M., S.G.-S. and M.P. were supported by the EMBL Interdisciplinary Postdoc programme under the Marie Sklodowska Curie Actions COFUND (grant numbers 291772 and 664726). L.M. is supported by the DFG (CMFI Cluster of Excellence EXC 2124 and Emmy Noether Program). C.V.G. is the recipient of an EMBO long-term postdoctoral fellowship and an add-on fellowship from the Christiane Nüsslein-Volhard-Stiftung. U.L. is supported by JPIAMR grant EMBARK. K.R.P. is supported by the UK Medical Research Council (MC_UU_00025/11). B.S. is supported by DFG CRC1371, ERC grant EVOGUTHEALTH (ID 865615), DZIF and CEGIMIR.

Author contributions This study was conceived by K.R.P., P.B. and A.T.; designed by L.M., C.V.G., M.P. and A.T.; and supervised by L.M., M.Z., B.S., G.Z., P.B. and A.T. L.M., M.P., T.B. and E.E.A. conducted MIC measurements. C.V.G. performed the bactericidal/bacteriostatic experiments. L.M., C.V.G., C.E., P.M., S.G.S., E.C., B.Z. and C.G. performed the antidote experiments (L.M., P.M., E.C. and C.G. the screen and in vitro validation; C.V.G., P.M. and S.G.-S. the community experiments; and L.M., C.E. and B.Z. the mouse experiments). Data pre-processing, curation and comparisons to databases were performed by J.W., M.K., A.M., U.L. and S.K.F. Data interpretation was performed by L.M., C.V.G., J.W., M.Z., B.S., G.Z. and A.T. L.M., C.V.G. and A.T. wrote the manuscript with feedback from all authors. L.M., C.V.G., J.W. and M.K. designed the figures with input from G.Z. and A.T. All authors approved the final version for publication.

Competing interests EMBL has filed a patent on using the antidotes identified in this study for prevention and/or treatment of dysbiosis and for microbiome protection (European patent application no. EP19216548.8). L.M., C.V.G., E.C. and A.T. are listed as inventors.

Additional information

Supplementary information The online version contains supplementary material available at https://doi.org/10.1038/s41586-021-03986-2.

Correspondence and requests for materials should be addressed to Lisa Maier or Athanasios Typas.

Peer review information *Nature* thanks Gerry Wright and the other, anonymous, reviewer(s) for their contributions to the peer review of this work.

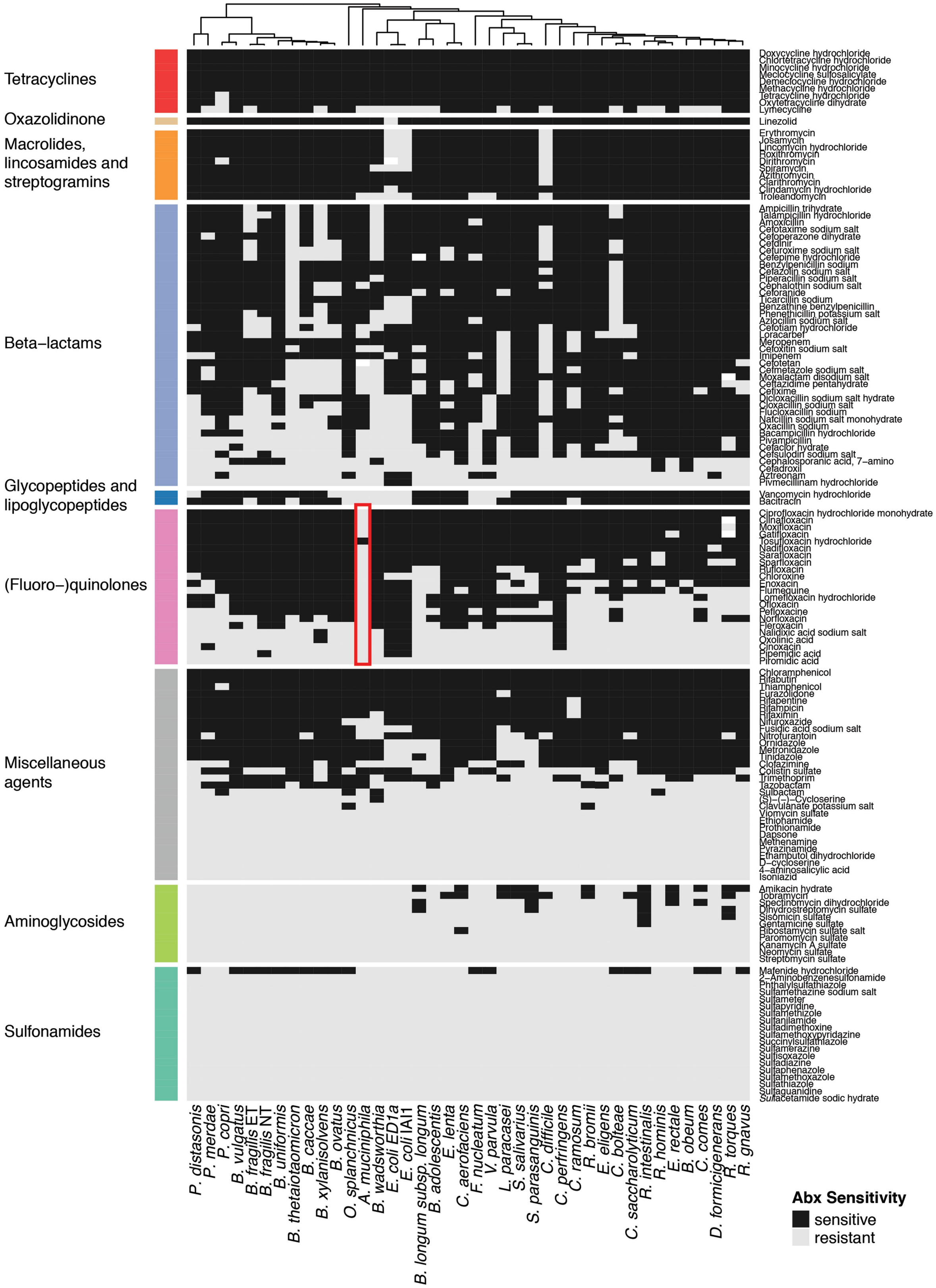

Extended Data Fig. 1 | Effects of 144 antibiotics on 40 human gut commensals. Heat map according to sensitivity or resistance of each strain to the respective antibiotic at a concentration of 20 μM. Antibiotics are grouped according to drug classes and species are clustered according to their responses across the 144 antibiotics tested. Data is replotted from[2]. Of note, *Akkermansia muciniphila*, a species associated with protection against different diseases and dysbiotic states[62], and even positive responses to immunotherapy[63], is resistant to nearly all quinolone antibiotics (red box). We consolidated this finding by MIC determination for Ciprofloxacin (>32 μg/ml), Gatifloxacin (>32 μg/ml), Moxifloxacin (>32 μg/ml), Norfloxacin (>256 μg/ml) and Ofloxacin (>32 μg/ml).

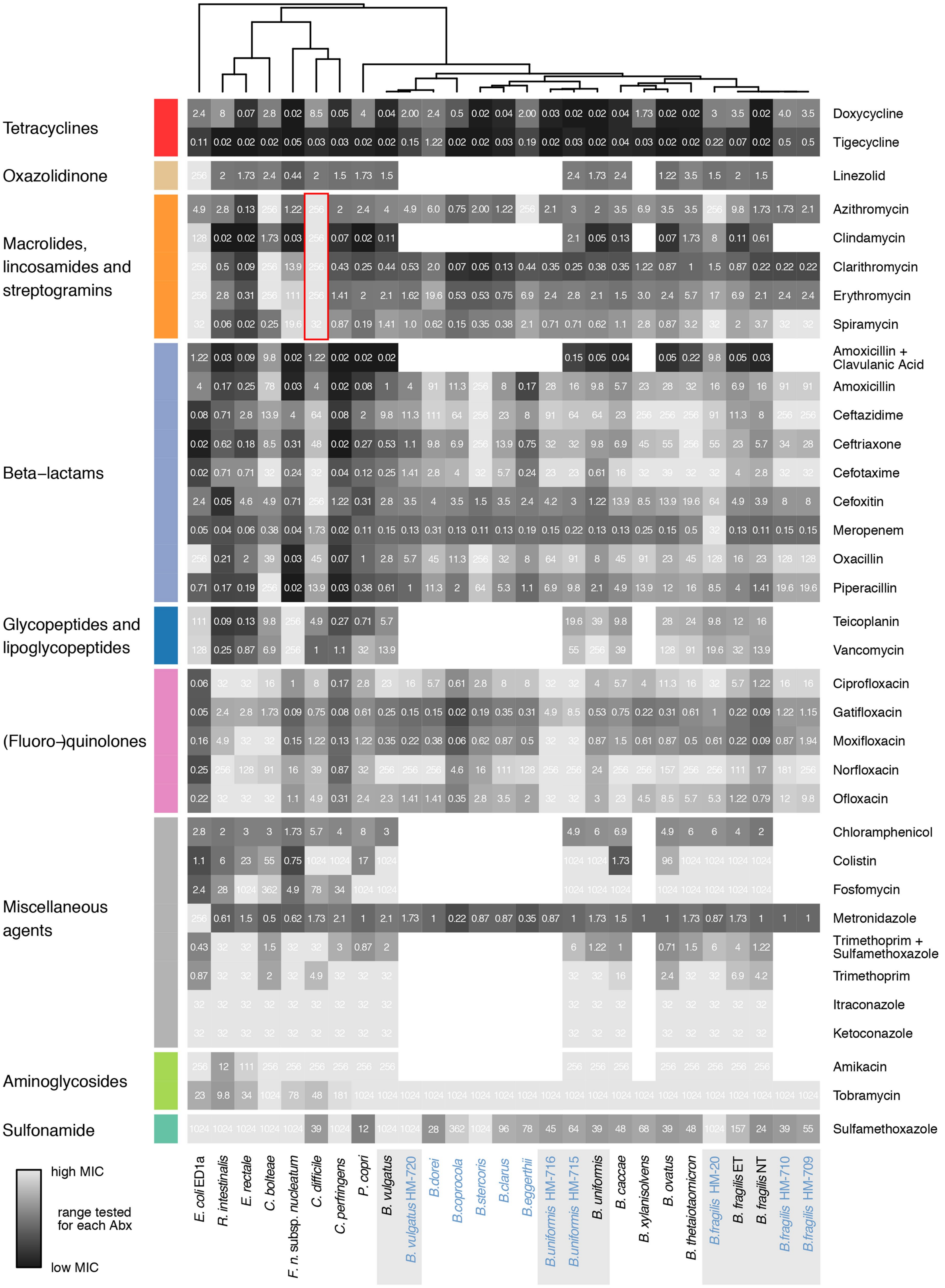

		E. coli ED1a	R. intestinalis	E. rectale	C. bolteae	F. n. subsp. nucleatum	C. difficile	C. perfringens	P. copri	B. vulgatus	B. vulgatus HM-720	B.dorei	B.coprocola	B.stercoris	B.clarus	B.eggerthii	B.uniformis HM-716	B.uniformis HM-715	B. uniformis	B. caccae	B. xylanisolvens	B. ovatus	B. thetaiotaomicron	B.fragilis HM-20	B. fragilis ET	B. fragilis NT	B.fragilis HM-710	B.fragilis HM-709
Tetracyclines	Doxycycline	2.4	8	0.07	2.8	0.02	8.5	0.05	4	0.04	2.00	2.4	0.5	0.02	0.04	2.00	0.03	0.02	0.02	0.04	1.73	0.02	0.02	3	3.5	0.02	4.0	3.5
	Tigecycline	0.11	0.02	0.02	0.02	0.05	0.03	0.03	0.02	0.02	0.15	1.22	0.02	0.02	0.03	0.19	0.02	0.03	0.02	0.04	0.03	0.02	0.02	0.22	0.07	0.02	0.5	0.5
Oxazolidinone	Linezolid	256	2	1.73	2.4	0.44	2	1.5	1.73	1.5								2.4	1.73	2.4		1.22	3.5	1.5	2	1.5		
Macrolides, lincosamides and streptogramins	Azithromycin	4.9	2.8	0.13	256	1.22	256	2	2.4	4	4.9	6.0	0.75	2.00	1.22	256	2.1	3	2	3.5	6.9	3.5	3.5	256	9.8	1.73	1.73	2.1
	Clindamycin	128	0.02	0.02	1.73	0.03	256	0.07	0.02	0.11								2.1	0.05	0.13		0.07	1.73	8	0.11	0.61		
	Clarithromycin	256	0.5	0.09	256	13.9	256	0.43	0.25	0.44	0.53	2.0	0.07	0.05	0.13	0.44	0.35	0.25	0.38	0.35	1.22	0.87	1	1.5	0.87	0.22	0.22	0.22
	Erythromycin	256	2.8	0.31	256	111	256	1.41	2	2.1	1.62	19.6	0.53	0.53	0.75	6.9	2.4	2.8	2.1	1.5	3.0	2.4	5.7	17	6.9	2.1	2.4	2.4
	Spiramycin	32	0.06	0.02	0.25	19.6	32	0.87	0.19	1.41	1.0	0.62	0.15	0.35	0.38	2.1	0.71	0.71	0.62	1.1	2.8	0.87	3.2	32	2	3.7	32	32
Beta–lactams	Amoxicillin + Clavulanic Acid	1.22	0.03	0.09	9.8	0.02	1.22	0.02	0.02	0.02								0.15	0.05	0.04		0.05	0.22	9.8	0.05	0.03		
	Amoxicillin	4	0.17	0.25	78	0.03	4	0.02	0.08	1	4	91	11.3	256	8	0.17	28	16	9.8	5.7	23	28	32	16	6.9	16	91	91
	Ceftazidime	0.08	0.71	2.8	13.9	4	64	0.08	2	9.8	11.3	111	64	256	23	8	91	64	64	23	256	256	256	91	11.3	8	256	256
	Ceftriaxone	0.02	0.62	0.18	8.5	0.31	48	0.02	0.27	0.53	1.1	9.8	6.9	256	13.9	0.75	32	32	9.8	6.9	45	55	256	55	23	5.7	34	28
	Cefotaxime	0.02	0.71	0.71	32	0.24	32	0.04	0.12	0.25	1.41	2.8	4	32	5.7	0.24	23	23	0.61	16	32	39	32	32	4	2.8	32	32
	Cefoxitin	2.4	0.05	4.6	4.9	0.71	256	1.22	0.31	2.8	3.5	4	3.5	1.5	3.5	2.4	4.2	3	1.22	13.9	8.5	13.9	19.6	64	4.9	3.9	8	8
	Meropenem	0.05	0.04	0.06	0.38	0.04	1.73	0.02	0.11	0.15	0.13	0.31	0.13	0.11	0.13	0.19	0.15	0.22	0.13	0.13	0.25	0.15	0.5	32	0.13	0.11	0.15	0.15
	Oxacillin	256	0.21	2	39	0.03	45	0.07	1	2.8	5.7	45	11.3	256	32	8	64	91	8	45	91	23	45	128	16	23	128	128
	Piperacillin	0.71	0.17	0.19	256	0.02	13.9	0.03	0.38	0.61	1	11.3	2	64	5.3	1.1	6.9	9.8	2.1	4.9	13.9	12	16	8.5	4	1.41	19.6	19.6
Glycopeptides and lipoglycopeptides	Teicoplanin	111	0.09	0.13	9.8	256	4.9	0.27	0.71	5.7								19.6	39	9.8		28	24	9.8	12	16		
	Vancomycin	128	0.25	0.87	6.9	256	1	1.1	32	13.9								55	256	39		128	91	19.6	32	13.9		
(Fluoro-)quinolones	Ciprofloxacin	0.06	32	32	16	1	8	0.17	2.8	23	16	5.7	0.61	2.8	8	8	32	32	4	5.7	4	11.3	16	32	5.7	1.22	16	16
	Gatifloxacin	0.05	2.4	2.8	1.73	0.09	0.75	0.08	0.61	0.25	0.15	0.15	0.02	0.19	0.35	0.31	4.9	8.5	0.53	0.75	0.22	0.31	0.61	1	0.22	0.09	1.22	1.15
	Moxifloxacin	0.16	4.9	32	32	0.15	1.22	0.13	1.22	0.35	0.22	0.38	0.06	0.62	0.87	0.5	32	32	0.87	1.5	0.61	0.87	0.5	0.61	0.22	0.09	0.87	1.94
	Norfloxacin	0.25	256	128	91	16	39	0.87	32	256	256	256	4.6	16	111	128	256	256	24	256	256	157	256	256	111	17	181	256
	Ofloxacin	0.22	32	32	32	1.1	4.9	0.31	2.4	2.3	1.41	1.41	0.35	2.8	3.5	2	32	32	3	23	4.5	8.5	5.7	5.3	1.22	0.79	12	9.8
Miscellaneous agents	Chloramphenicol	2.8	2	3	3	1.73	5.7	4	8	3								4.9	6	6.9		4.9	6	6	4	2		
	Colistin	1.1	6	23	55	0.75	1024	1024	17	1024								1024	1024	1.73		96	1024	1024	1024	1024		
	Fosfomycin	2.4	28	1024	362	4.9	78	34	1024	1024								1024	1024	1024		1024	1024	1024	1024	1024		
	Metronidazole	256	0.61	1.5	0.5	0.62	1.73	2.1	1	2.1	1.73	1	0.22	0.87	0.87	0.35	0.87	1	1.73	1.5	1	1	1.73	0.87	1.73	1	1	1
	Trimethoprim + Sulfamethoxazole	0.43	32	32	1.5	32	32	3	0.87	2								6	1.22	1		0.71	1.5	6	4	1.22		
	Trimethoprim	0.87	32	32	2	32	4.9	32	32	32								32	32	16		2.4	32	32	6.9	4.2		
	Itraconazole	32	32	32	32	32	32	32	32	32								32	32	32		32	32	32	32	32		
	Ketoconazole	32	32	32	32	32	32	32	32	32								32	32	32		32	32	32	32	32		
Aminoglycosides	Amikacin	256	12	111	256	256	256	256	256	256								256	256	256		256	256	256	256	256		
	Tobramycin	23	9.8	34	1024	78	48	181	1024	1024	1024	1024	1024	1024	1024	1024	1024	1024	1024	1024	1024	1024	1024	1024	1024	1024	1024	1024
Sulfonamide	Sulfamethoxazole	1024	1024	1024	1024	1024	39	1024	12	1024	1024	28	362	1024	96	78	45	64	39	48	68	39	48	1024	157	24	39	55

Extended Data Fig. 2 | MICs for 20 species/27 strains on 35 antimicrobials. Heat map depicts MICs for each drug-strain pair in µg/ml. Heat map color gradient is adjusted to the MICs concentration range tested on the respective MIC test strip. Black depicts sensitivity and light grey resistance. Mean values across two biological replicates are shown (Suppl. Table 4). The species/strains from the screen are shown in black, additional strains to investigate intraspecies and intragenus variation within the *Bacteroides* genus are shown in blue. The grey background indicates that several strains per species were tested. Of note, *C. difficile* is particularly resistant to all tested macrolides and clindamycin (red box).
"

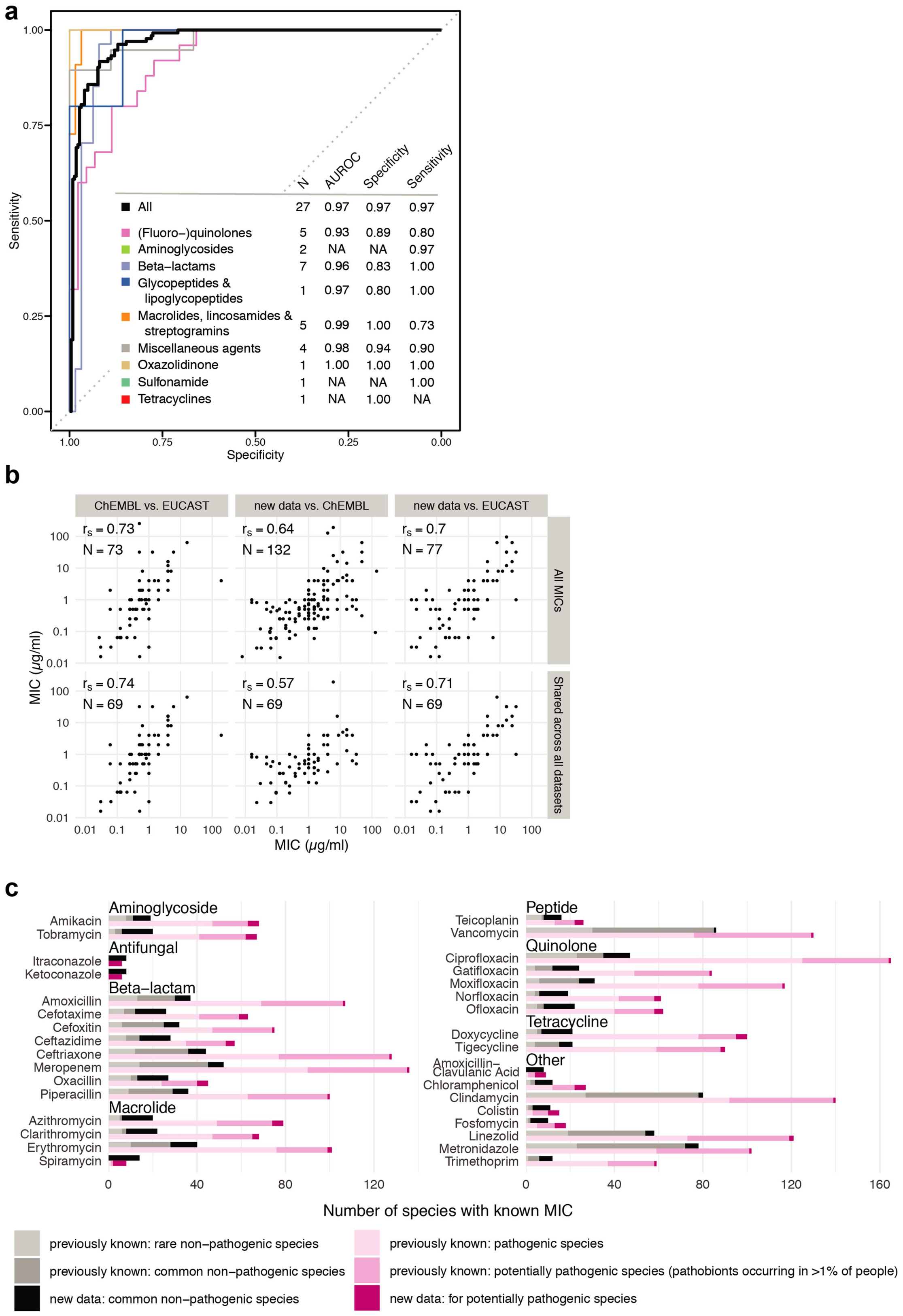

Extended Data Fig. 3 | See next page for caption.

Extended Data Fig. 3 | MIC dataset validates antibiotic sensitivity profiles from the screen and is consistent with publicly available MICs. a. Receiver operating characteristic (ROC) curve analysis was performed to evaluate sensitivity and specificity of the screen[2] using the MIC dataset. Results from the screen were considered as validated if MICs were below/above the 20 µM antibiotic concentration that was tested in the screen (allowing a twofold error margin). N is the number of antibiotics that we tested both in the screen and determined MICs for; AUROC is the area under the characteristic ROC. TN denotes true negatives, FP false positives, TP true positives, FN false negatives. **b**. Comparison including Spearman correlation coefficients of the MICs from this study to MICs from the ChEMBL[19] and EUCAST[16] databases. Panels in the upper row: comparison between all MICs that are shared between the two indicated datasets. Panels in the lower row: comparison of the 69 MICs that are shared across all three datasets. Despite experimental differences, our MICs correlate well with available EUCAST/ ChEMBL data. **c**. Number of the sum of new (this study) and already available MICs (EUCAST/ ChEMBL) per drug according to antibiotic class and prevalence/virulence of the bacterial species. The new dataset expands MICs across the board and specifically fills the knowledge gap on non-pathogenic species.

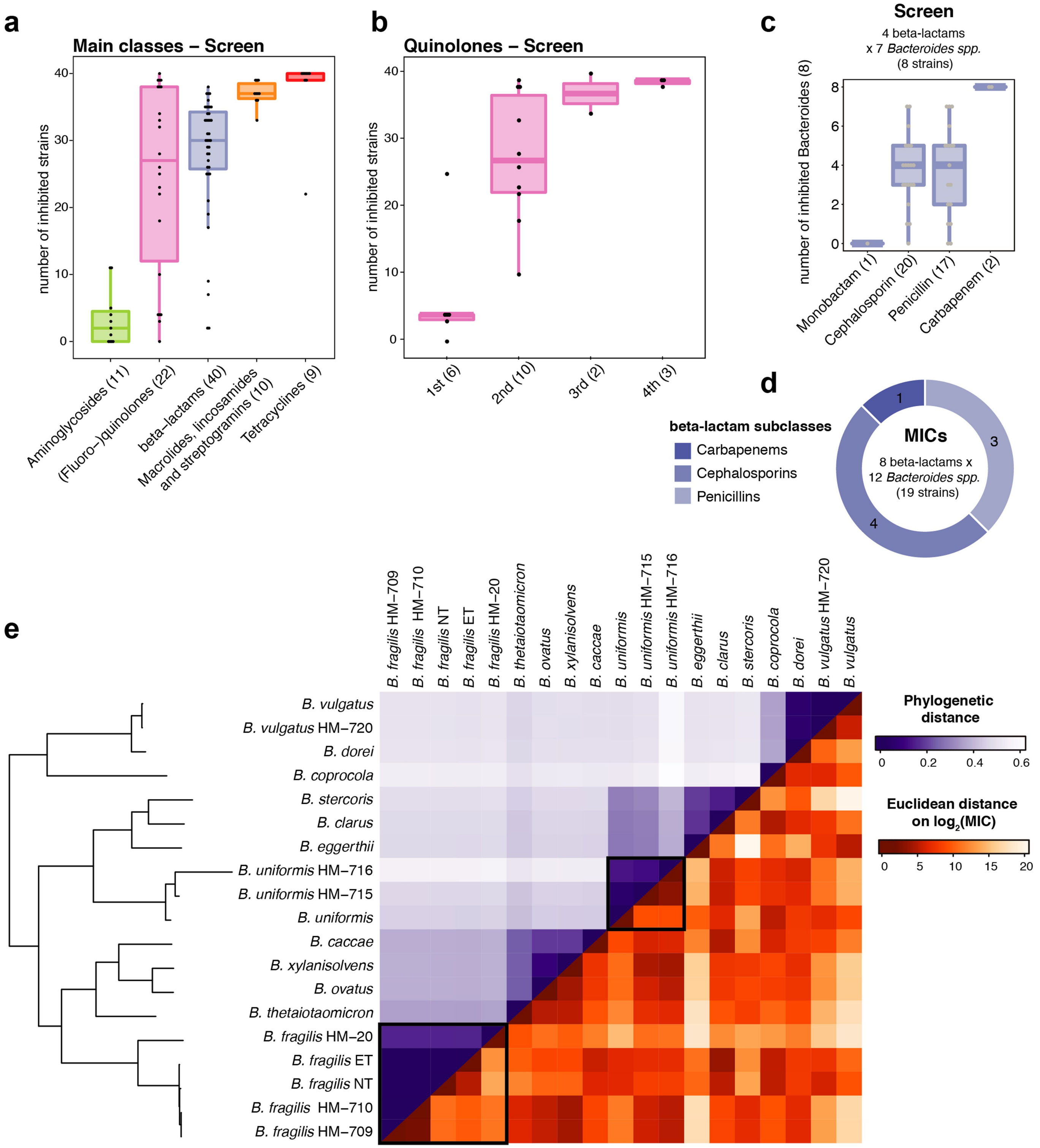

Extended Data Fig. 4 | Antibiotic classes exhibit distinct behaviours in gut bacterial species. a. Number of inhibited strains per antibiotic class (number of tested drugs per class in brackets). In total 40 strains were tested at a 20 µM antibiotic concentration. Boxes span the IQR and whiskers extend to the most extreme data points up to a max of 1.5 times the IQR. **b**. Number of inhibited strains per (fluoro-)quinolone drug generation. Number of tested drugs per generation is indicated in brackets - boxplots as in **a**. **c**–**d**. Overview of the number of drugs tested per β-lactam subclasses on *Bacteroides* species (*spp*) in screen (**c**) and for MICs (**d**). **e**. Heat map of phylogenetic relationship between *Bacteroides spp* (upper triangular matrix) ordered by phylogeny and their resistance profiles across β-lactam antibiotics (lower triangular matrix). Colors represent the pairwise phylogenetic distance and the Euclidean distance on the log2 transformed MICs for β-lactams. Examples of strains from the same species (*B. fragilis* / *B. uniformis*) that respond differently to β-lactam antibiotics, are highlighted.

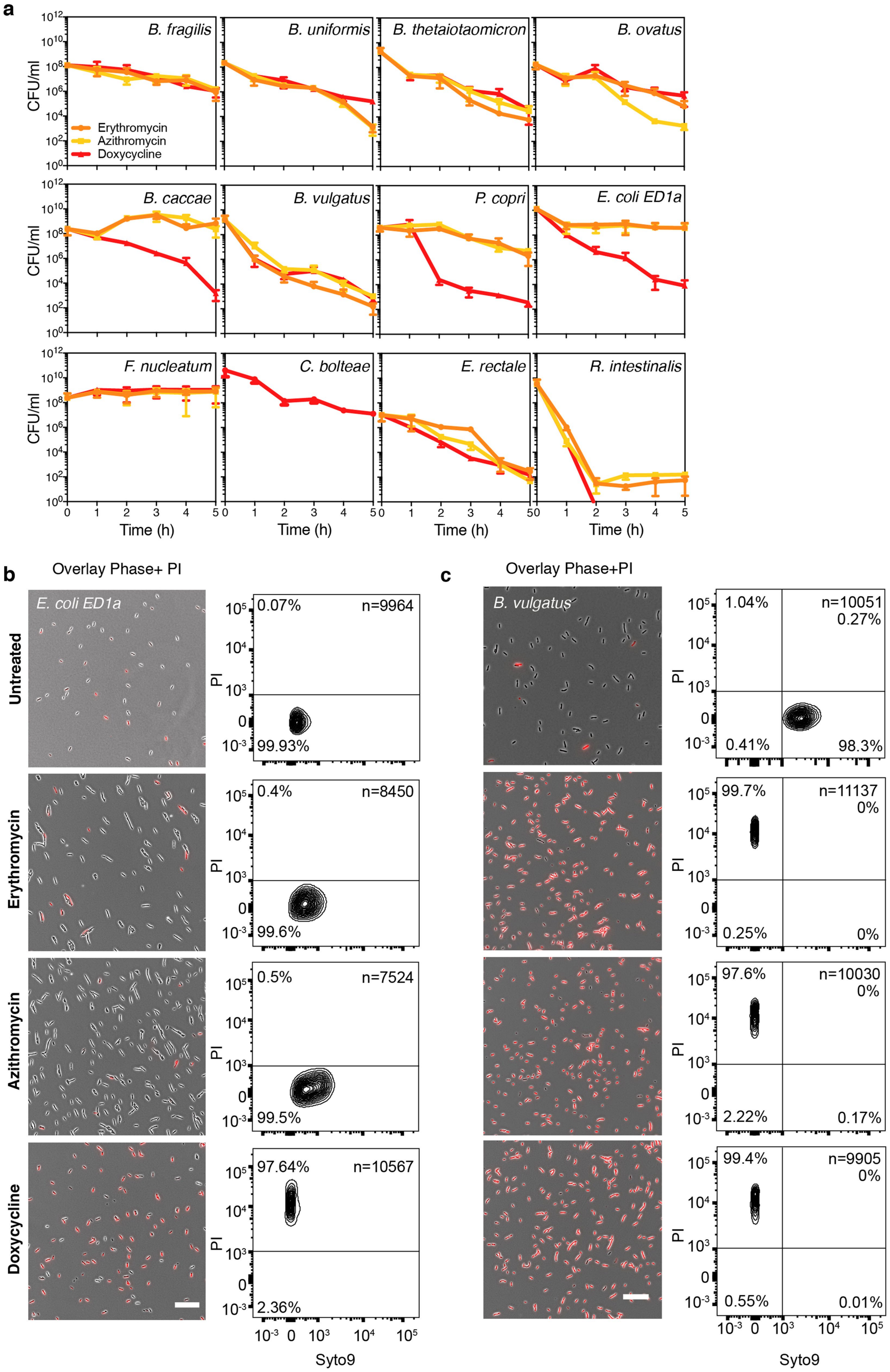

Extended Data Fig. 5 | Selective killing of macrolides and tetracyclines. **a**. Time-kill curves. The survival of 12 abundant gut microorganisms was assessed over a 5 h-treatment with either erythromycin, azithromycin or doxycycline. The graph shows the mean±SD of 3 independent experiments. **b**. Live/dead staining of macrolide or tetracycline-treated *E. coli* ED1a and *B. vulgatus*. The left panel shows an overlay of phase contrast and fluorescence microscopy images of propidium iodide (PI)-stained *E. coli* ED1a or *B. vulgatus* before and 5 h after erythromycin, azithromycin or doxycycline treatment. Cultures were concentrated before imaging; the scale bar is 10 µm. The right panel shows the corresponding quantification of live/dead-stained cells by flow cytometry with Syto9 on the x-axis (live cells) and PI on the y-axis (dead cells). As *E. coli* ED1a cells stain poorly with Syto9, we only quantified PI stained cells in this case. Both the total number of measured events (n) and the percentage of cells found in each region of the graph are indicated.

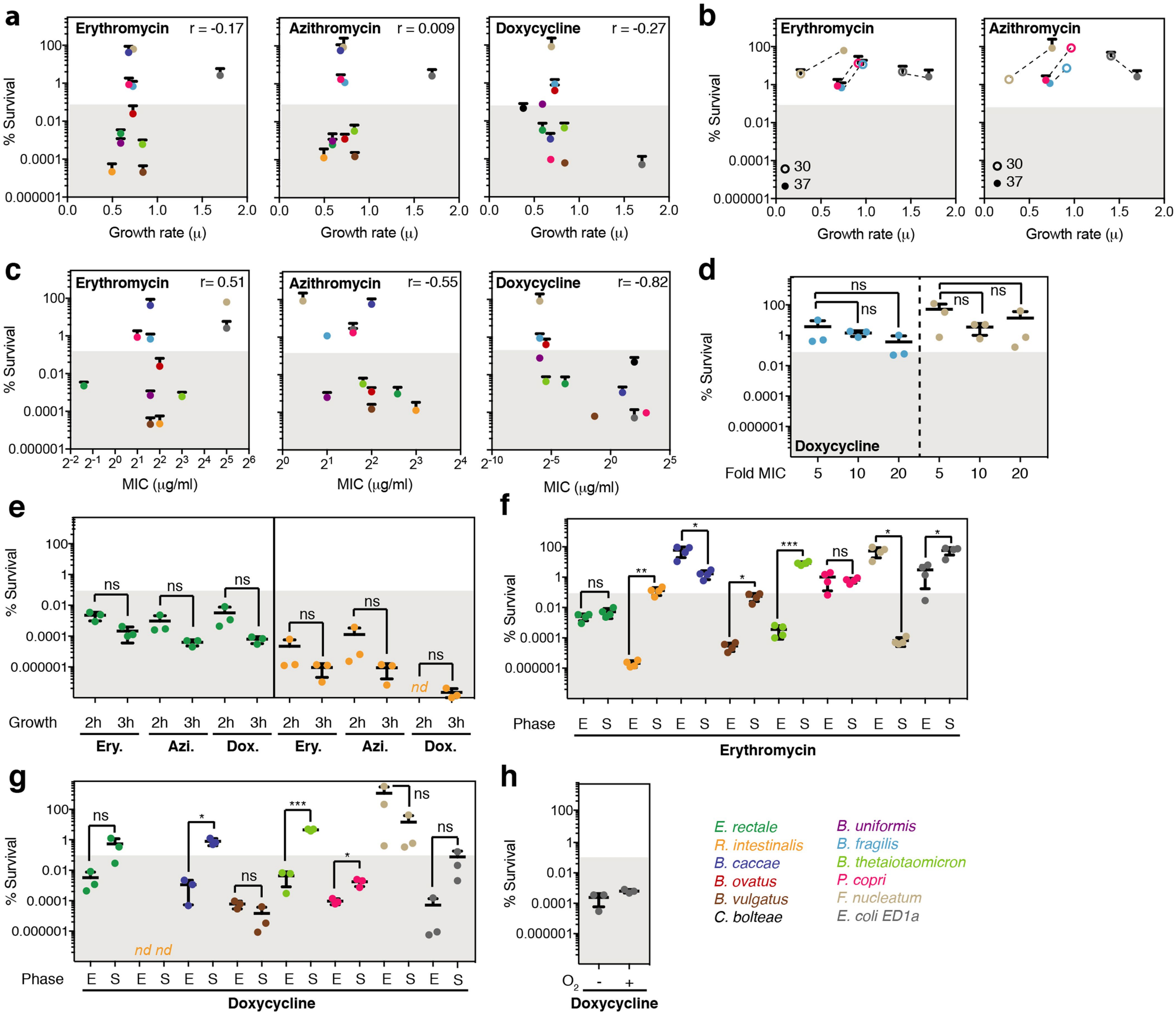

Extended Data Fig. 6 | Assessing potential confounding factors for the killing capacities of erythromycin, azithromycin and doxycycline. **a**. Scatter plot of individual bacterial specific growth rates (μ - hr^{-1}) and percentage survival after a 5-hour treatment with 5-fold MIC of erythromycin, azithromycin or doxycycline. *r* is the Spearman correlation coefficient. Tested species are color-coded here and, in all panels thereafter as indicated at the bottom of this figure. **b**. *B. fragilis* (blue), *F. nucleatum* (beige), *P. copri* (pink) and *E. coli* ED1a (grey) survival was assessed after a 5 h erythromycin and azithromycin treatment (5-fold MIC) at 30 °C (slow growth) and 37 °C (fast growth) - mean ±SD of three independent experiments. No monotonic trend was observed. **c**. Scatter plot of MICs and % survival after a 5 h treatment with 5-fold MIC of erythromycin, azithromycin or doxycycline. *r* is the Spearman correlation coefficient. Doxycycline exhibited a significant (*P* value = 0.0015) anti-correlation, i.e. more sensitive species to doxycycline (lower MIC) survived better when treated with antibiotic. Therefore, we tested further whether increasing the drug concentration in sensitive strains increased killing (panel d). **d**. *B. fragilis* (blue) and *F. nucleatum* (beige) survival after a 5-hour treatment as function of increasing doxycycline concentrations (mean ± SD of three independent experiments). No significant differences observed. In all cases doxycycline remained bacteriostatic. Significance calculated by unpaired two-sided t-test here and in all panels thereafter. **e**. To evaluate whether outgrowth from stationary phase affected our results, we selected two slow-growing strains, *E. rectale* (green) and *R. intestinalis* (orange) and grew them for 2 or 3 h after diluting from an overnight culture to an of OD_{578} 0.01. Both strains were then treated for 5 h with 5-fold MIC of erythromycin, azithromycin or doxycycline and their survival was assessed (mean ± SD of three independent experiments). Although 3 h grown cultures were killed slightly more effectively (difference is not statistically significant due to low number of replicates), this did not change the bactericidal or bacteriostatic characteristic of antibiotics. If anything, this means that we underestimate the killing for slow-growers, since all other experiments were performed with 2 h outgrowth. Nd: not detected (detection limit: 1 CFU/ml.). **f–g**. The survival of 8 selected gut microorganisms was measured after treating cells in exponential phase (E – 2h after dilution from an overnight culture) or in stationary phase (S – overnight growth) with 5-fold MIC of erythromycin (**f**) or doxycycline (**g**) for 5h (mean ± SD of three independent experiments). Consistent with the knowledge that antibiotic killing requires active growth, survival is higher in stationary phase for most strains (but not all – see *F. nucleatum*) that erythromycin or doxycycline kills. ns = non-significant; *, ** and *** denote *P* value <0.05, <0.01 and <0.001, respectively. nd as in e. **h**. *E. coli* ED1a survival was assessed after 5h treatment with 5-fold MIC of doxycycline in the presence or absence of oxygen. Killing was similar in both conditions.

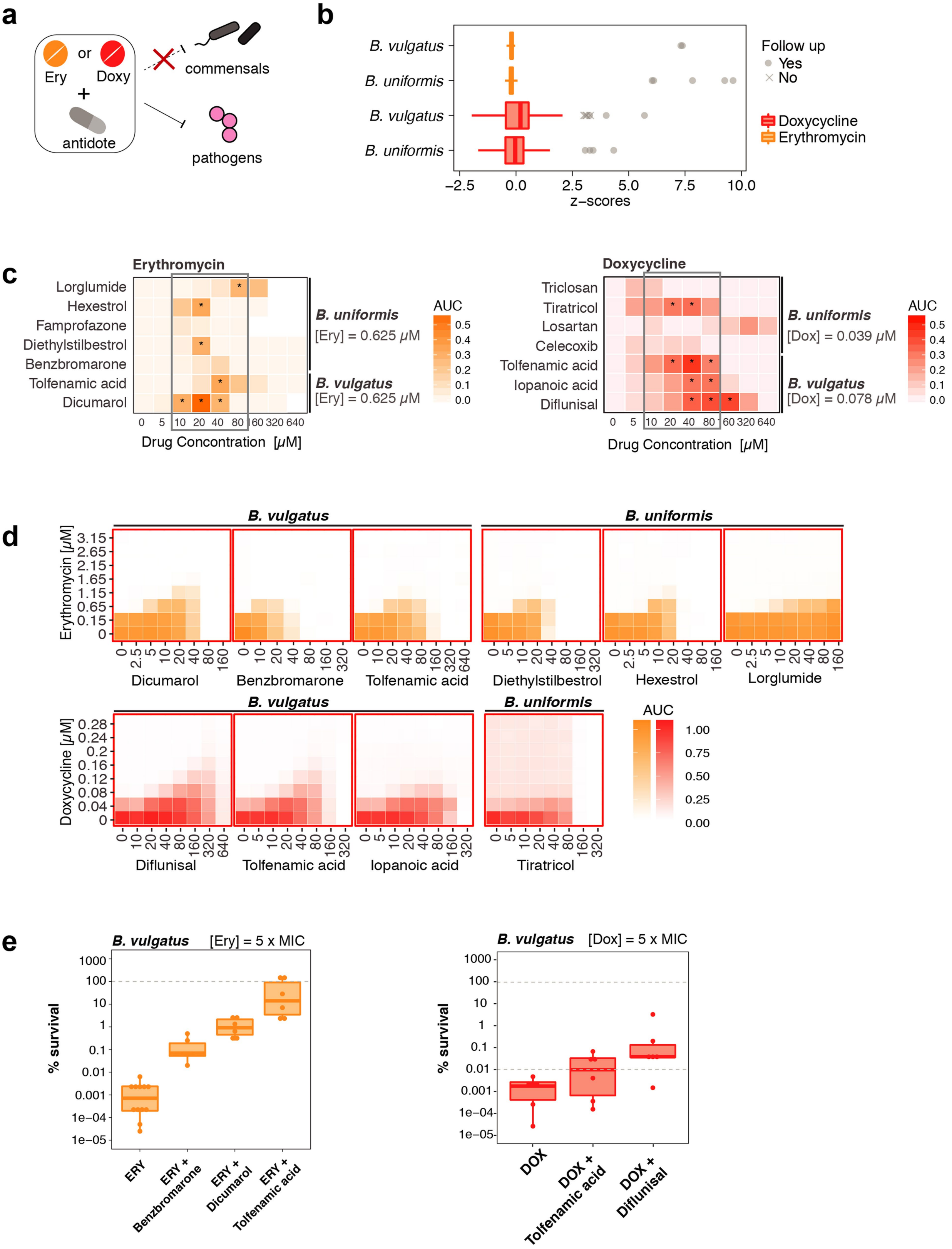

Extended Data Fig. 7 | See next page for caption.

Extended Data Fig. 7 | Identification and validation of macrolide and tetracycline antagonists (antidotes) in *B. vulgatus* and *B. uniformis*. **a**. Schematic illustration of combinatorial screen concept: searching for antidote compounds that antagonize the antibacterial effect of erythromycin or doxycycline on commensal but not on pathogenic bacteria. **b**. Z-scores on bacterial growth for combinatorial drug exposure with antibiotic and 1197 FDA-approved drugs of Prestwick library (2 replicates). Compounds that successfully protected *B. vulgatus* and/or *B. uniformis* in the presence of antibiotic (z-score > 3) are indicated in gray. The strongest hits (circles) were validated in concentration-dependent assays (**c**–**d**). Box plots as in Fig. 1c. **c**. Validation of the strongest antagonistic interactions in independent experiments. Erythromycin and doxycycline concentrations were kept constant for each species and concentration ranges were tested for antagonists. Asterisks indicate that at least 25% of the bacterial growth (compared to no drug controls) could be rescued by the antagonist at a given concentration. Heat map depicts median growth across triplicates. **d**. For 10 of the validated antagonists, 8 × 8 checkerboard assays were performed to define better the range of the antagonistic interaction. Heat maps depict bacterial growth based on normalized median of AUCs of 3–4 replicates. Antagonistic interactions are framed in red (all). **e**. Percentage of surviving *B. vulgatus* cells were determined after 5h incubation with either erythromycin (3.25 µM) or doxycycline (0.4 µM) alone or in presence of benzbromarone (40 µM), dicumarol (20 µM), tolfenamic acid (40 µM) or diflunisal (80 µM). Data is based on three independent experiments. Boxplots are plotted as in Fig. 1c.

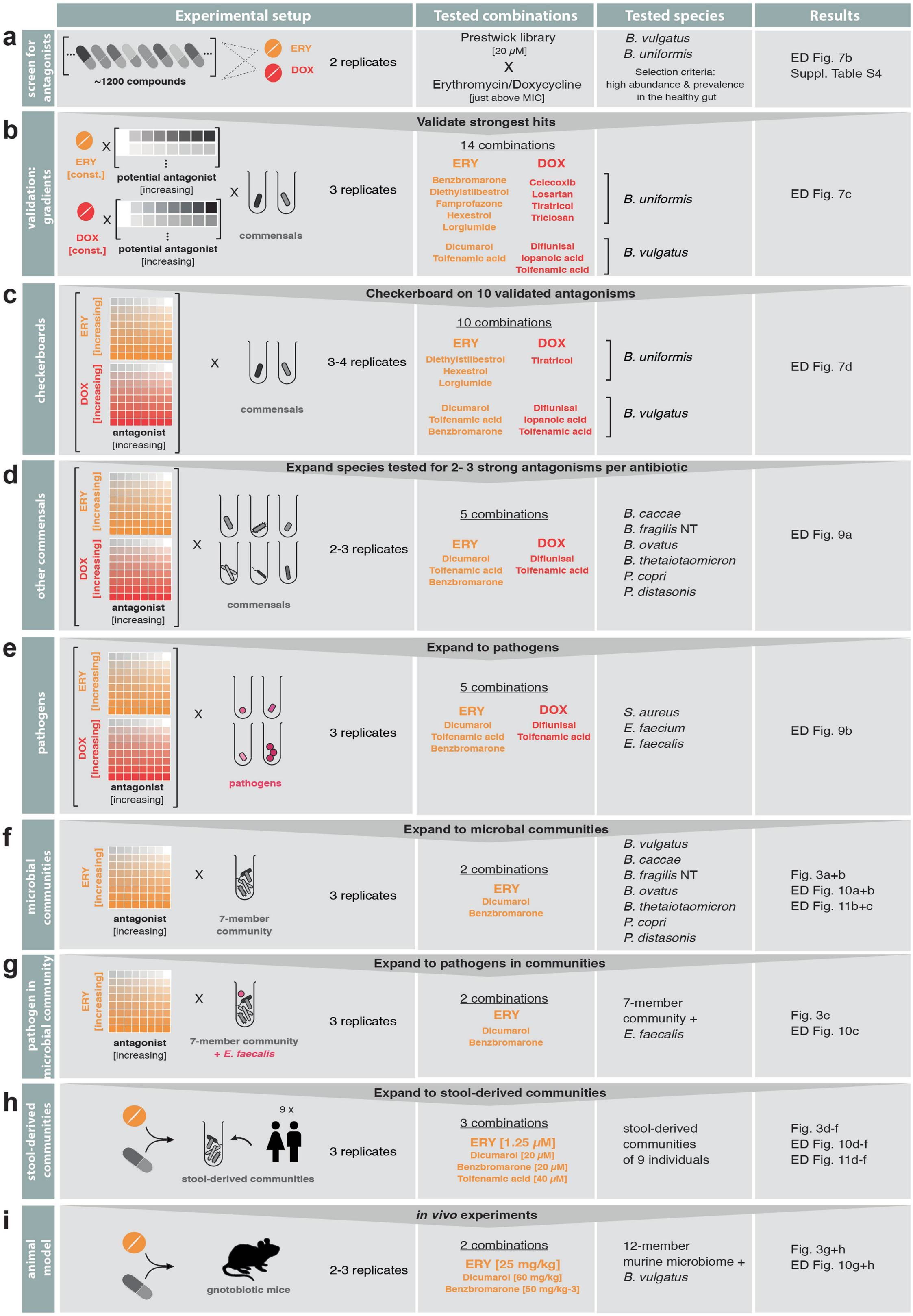

		Experimental setup		Tested combinations	Tested species	Results
a	screen for antagonists	~1200 compounds ERY DOX	2 replicates	Prestwick library [20 μM] X Erythromycin/Doxycycline [just above MIC]	*B. vulgatus* *B. uniformis* Selection criteria: high abundance & prevalence in the healthy gut	ED Fig. 7b Suppl. Table S4
b	validation: gradients	**Validate strongest hits** ERY [const.] X potential antagonist [increasing] DOX [const.] X potential antagonist [increasing] X commensals	3 replicates	14 combinations ERY: Benzbromarone, Diethylstilbestrol, Famprofazone, Hexestrol, Lorglumide; DOX: Celecoxib, Losartan, Tiratricol, Triclosan ERY: Dicumarol, Tolfenamic acid; DOX: Diflunisal, Iopanoic acid, Tolfenamic acid	*B. uniformis* *B. vulgatus*	ED Fig. 7c
c	checkerboards	**Checkerboard on 10 validated antagonisms** ERY [increasing] / DOX [increasing] antagonist [increasing] X commensals	3-4 replicates	10 combinations ERY: Diethylstilbestrol, Hexestrol, Lorglumide; DOX: Tiratricol ERY: Dicumarol, Tolfenamic acid, Benzbromarone; DOX: Diflunisal, Iopanoic acid, Tolfenamic acid	*B. uniformis* *B. vulgatus*	ED Fig. 7d
d	other commensals	**Expand species tested for 2- 3 strong antagonisms per antibiotic** ERY [increasing] / DOX [increasing] antagonist [increasing] X commensals	2-3 replicates	5 combinations ERY: Dicumarol, Tolfenamic acid, Benzbromarone DOX: Diflunisal, Tolfenamic acid	*B. caccae* *B. fragilis* NT *B. ovatus* *B. thetaiotaomicron* *P. copri* *P. distasonis*	ED Fig. 9a
e	pathogens	**Expand to pathogens** ERY [increasing] / DOX [increasing] antagonist [increasing] X pathogens	3 replicates	5 combinations ERY: Dicumarol, Tolfenamic acid, Benzbromarone DOX: Diflunisal, Tolfenamic acid	*S. aureus* *E. faecium* *E. faecalis*	ED Fig. 9b
f	microbial communities	**Expand to microbal communities** ERY [increasing] antagonist [increasing] X 7-member community	3 replicates	2 combinations ERY Dicumarol Benzbromarone	*B. vulgatus* *B. caccae* *B. fragilis* NT *B. ovatus* *B. thetaiotaomicron* *P. copri* *P. distasonis*	Fig. 3a+b ED Fig. 10a+b ED Fig. 11b+c
g	pathogen in microbial community	**Expand to pathogens in communities** ERY [increasing] antagonist [increasing] X 7-member community + *E. faecalis*	3 replicates	2 combinations ERY Dicumarol Benzbromarone	7-member community + *E. faecalis*	Fig. 3c ED Fig. 10c
h	stool-derived communities	**Expand to stool-derived communities** 9 x stool-derived communities	3 replicates	3 combinations ERY [1.25 μM] Dicumarol [20 μM] Benzbromarone [20 μM] Tolfenamic acid [40 μM]	stool-derived communities of 9 individuals	Fig. 3d-f ED Fig. 10d-f ED Fig. 11d-f
i	animal model	***in vivo* experiments** gnotobiotic mice	2-3 replicates	2 combinations ERY [25 mg/kg] Dicumarol [60 mg/kg] Benzbromarone [50 mg/kg-3]	12-member murine microbiome + *B. vulgatus*	Fig. 3g+h ED Fig. 10g+h

Extended Data Fig. 8 | Schematic overview of screen for microbiome-protective antibiotic antidotes. Workflow with decision process on which erythromycin and doxycycline antagonists to move to next evaluation step.

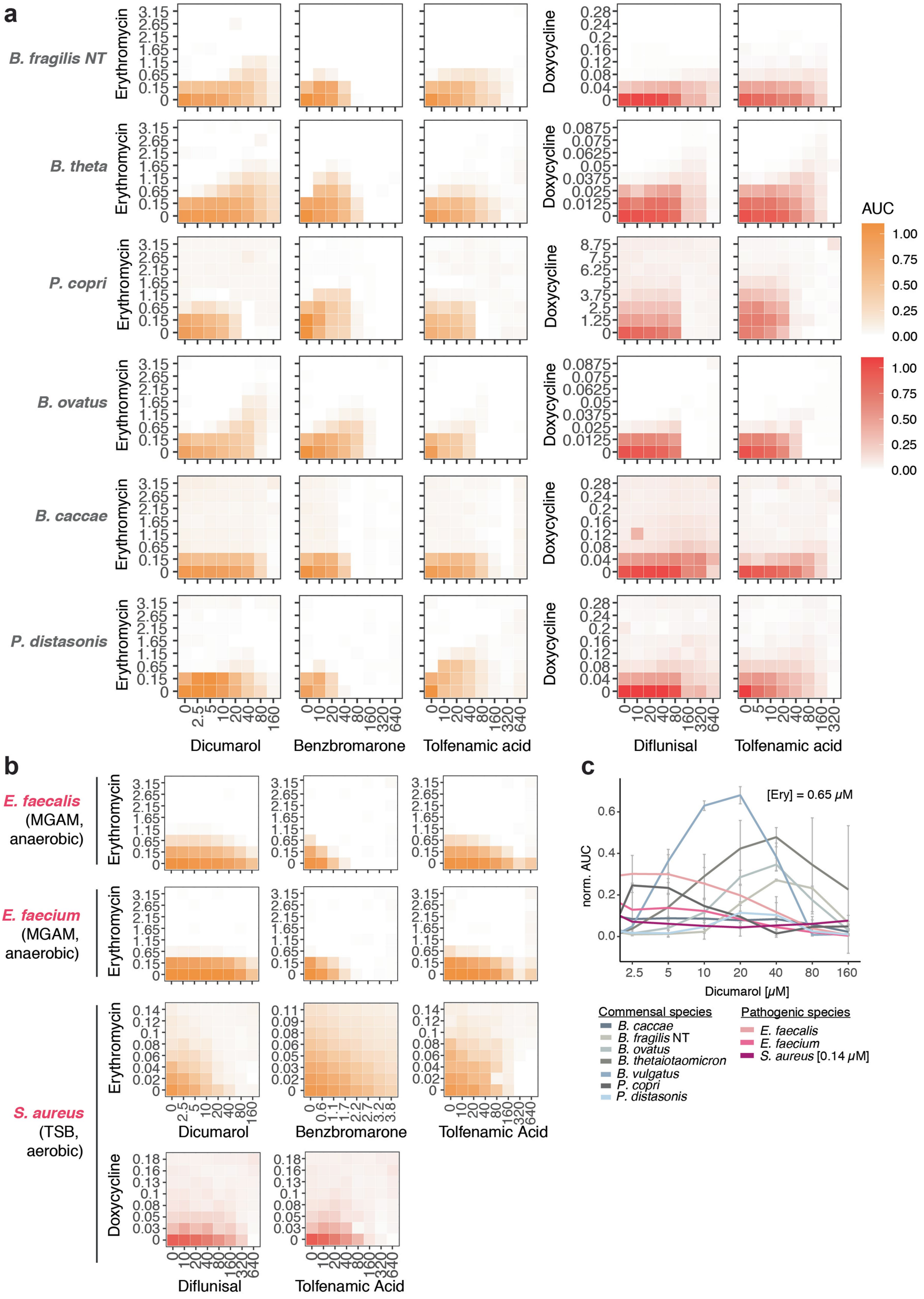

Extended Data Fig. 9 | See next page for caption.

Extended Data Fig. 9 | Antidotes work on further gut commensals, but do not compromise antibiotic efficacy on relevant pathogens. a. 8 × 8 checkerboard assays to investigate if antidote is also protective for additional gut commensals. All combinations were tested in MGAM medium under anaerobic conditions. Heat map depicts bacterial growth based on median AUCs from 2–3 independent replicates. Concentrations are stated in µM. **b**. 8 × 8 checkerboard assays to evaluate antidote effects on the activity of erythromycin and doxycycline in relevant pathogenic species. The gastrointestinal pathogens *E. faecalis* and *E. faecium* were tested under anaerobic conditions. *S. aureus*, a cause of extra-intestinal infections, such as bacteremia and infective endocarditis, was tested under aerobic conditions. Heatmaps depict mean normalized AUCs of three biological replicates. Antidotes exhibit either neutral or even slight synergistic effects with antibiotics. **c**. Dicumarol rescues commensal growth (n = 2, anaerobic conditions) in a concentration-dependent manner. Erythromycin still retains its activity against pertinent pathogens such as *E. faecium*, *E. faecalis* (n = 3, anaerobic conditions) and *S. aureus* (n = 3, aerobic conditions) - see Suppl. Table 1 for strains used. 0.65 µM (~0.5 µg/ml) erythromycin is within range of the MIC breakpoints for *Staphylococcus* (1 µg/ml) and *Streptococci* groups A, B, C & G (0.25 µg/ml). Error bars depict standard deviation.

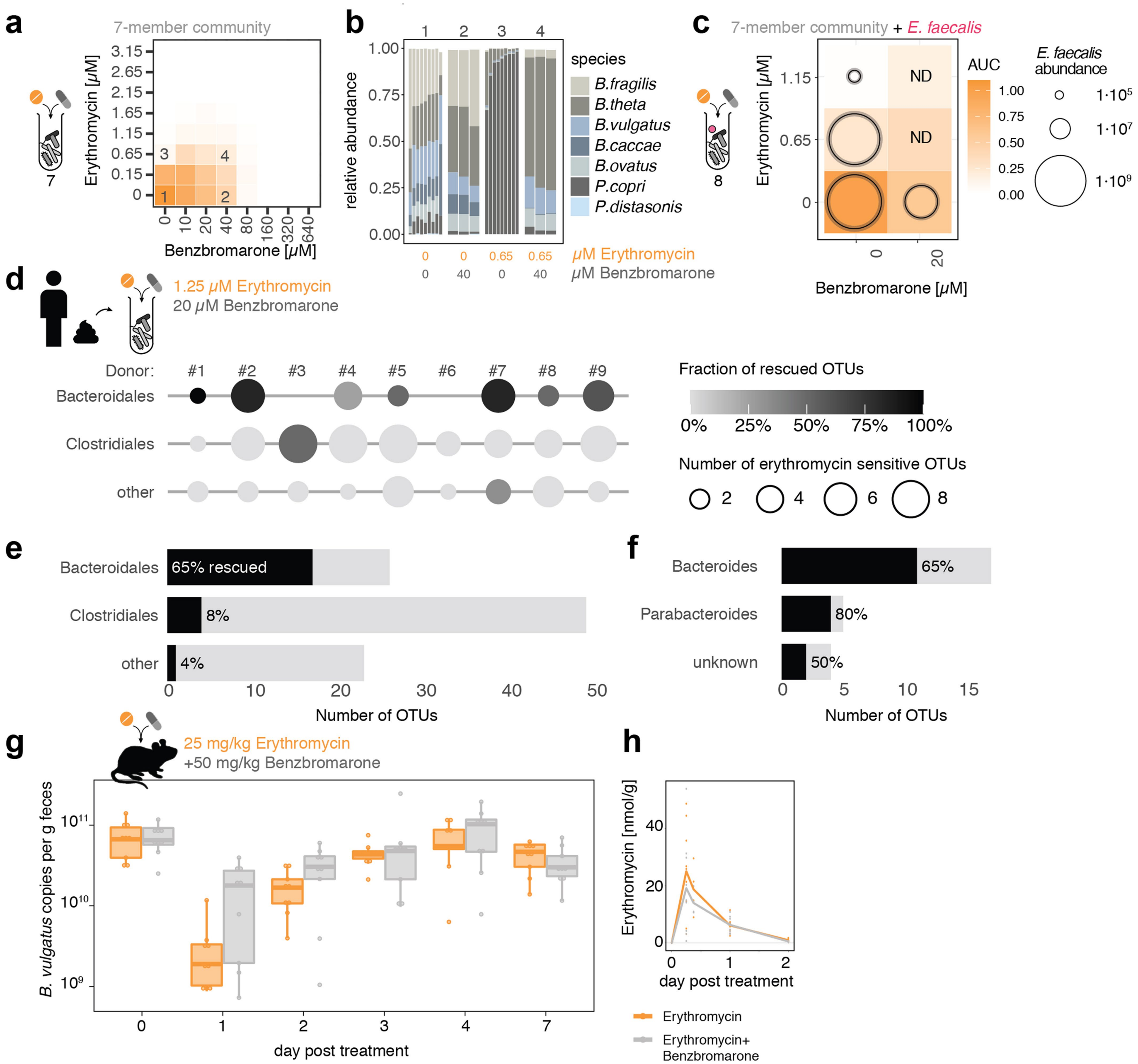

Extended Data Fig. 10 | The antidote benzbromarone selectively protects *Bacteroides* species from erythromycin in microbial communities. a. The same 7-member synthetic gut microbial community as in Fig. 3a can be protected from erythromycin by the antidote benzbromarone. Heatmaps depict median bacterial growth based on normalized AUCs of the community of three replicates. **b.** Community compositions in selected erythromycin-benzbromarone concentration combinations (1–4 referring to checkerboard tiles in **a**) demonstrate that benzbromarone alone does not alter the community structure, but rescues some *Bacteroides* species and largely the community composition from erythromycin treatment. Depicted as in Fig. 3b - control and erythromycin alone experiments same as in Fig. 3b. **c.** When the Bacteroidales community contains the pathogen *E. faecalis*, benzbromarone rescues community growth upon erythromycin treatment, but enhances the ability of erythromycin to target *E. faecalis*. Plotted as in Fig. 3c. **d**–**f.** In complex human-stool derived communities from nine healthy donors (column #1 – 9), benzbromarone protects 65% of Bacteroidales OTUs from erythromycin, and at least one sensitive Bacteroidales OTU per individual (2 biological × 2 technical replicates). Plotted as in Fig. 3d. The fractions of rescued OTUs per order (**e**) and for Bacteroidales OTUs per genus (**f**) across all nine donors indicate that primarily *Bacteroides* species are rescued. **g.** In gnotobiotic mice colonized with a defined 12-member mouse microbiome[31] and *B. vulgatus*, administration of benzbromarone slightly (albeit not significantly, two-sided Mann-Whitney U test) mitigates the temporal decrease in fecal *B. vulgatus* counts that erythromycin causes. Mice received a single oral dose of erythromycin (N = 9) or erythromycin + benzbromarone (N = 9) in two independent experiments. Data of the erythromycin-treated group is partially overlapping with data shown in Fig. 3g as experiments were conducted in parallel. Boxes are plotted as in Fig. 1c. **h.** Both groups of mice show similar faecal erythromycin concentrations over the course of the experiment shown in **g**.

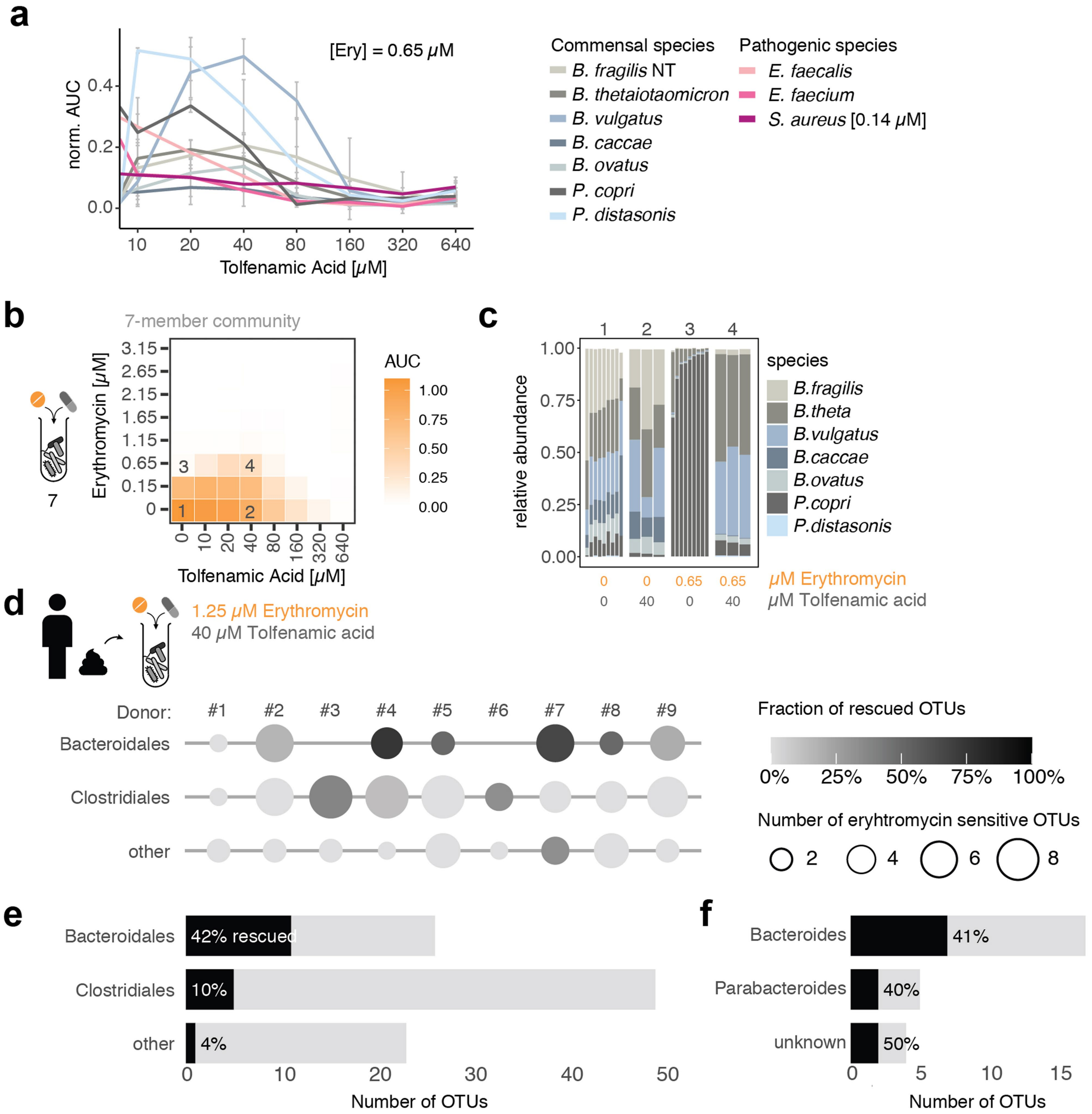

Extended Data Fig. 11 | The antidote tolfenamic acid protects *Bacteroides* species from erythromycin in microbial communities. a. Tolfenamic acid rescues commensal growth (based on median AUCs, N = 2) at clinical relevant erythromycin concentrations in a concentration-dependent manner (anaerobic conditions). Erythromycin still retains its activity against pertinent pathogens such as *E. faecium*, *E. faecalis* (based on median AUCs, N = 3, anaerobic conditions) and *S. aureus* ([erythromycin] = 0.14 μM, N = 3, aerobic conditions). Error bars depict standard deviation. **b**. The same 7-member synthetic gut microbial community as in Fig. 3a can be protected from erythromycin by the tolfenamic acid. Heat maps depict median bacterial growth based on normalized AUCs of the community of 3 replicates. **c**. Community compositions in selected erythromycin-tolfenamic acid concentration combinations (1–4 referring to checkerboard tiles in **b**) demonstrate that tolfenamic acid alone does not alter the community structure, but rescues some *Bacteroides* species and largely the community composition from erythromycin treatment. Depicted as in Fig. 3b – control and erythromycin alone experiments same as in Fig. 3b. **d**–**f**. In complex human-stool derived communities from 9 healthy donors (column #1 – 9), tolfenamic acid can rescue 42% of the erythromycin-sensitive Bacteroidales OTUs (2 biological × 2 technical replicates). Data is plotted as in Fig. 3d. Bars depict the absolute numbers of erythromycin-sensitive OTUs and the percentage of rescued OTUs per order (**e**) or genus (**f**) across all nine individuals.

nature research

Corresponding author(s): Lisa Maier, Athansios Typas

Last updated by author(s): Aug 10, 2021

Reporting Summary

Nature Research wishes to improve the reproducibility of the work that we publish. This form provides structure for consistency and transparency in reporting. For further information on Nature Research policies, see our Editorial Policies and the Editorial Policy Checklist.

Statistics

For all statistical analyses, confirm that the following items are present in the figure legend, table legend, main text, or Methods section.

n/a	Confirmed	
☐	☒	The exact sample size (*n*) for each experimental group/condition, given as a discrete number and unit of measurement
☐	☒	A statement on whether measurements were taken from distinct samples or whether the same sample was measured repeatedly
☐	☒	The statistical test(s) used AND whether they are one- or two-sided *Only common tests should be described solely by name; describe more complex techniques in the Methods section.*
☒	☐	A description of all covariates tested
☐	☒	A description of any assumptions or corrections, such as tests of normality and adjustment for multiple comparisons
☐	☒	A full description of the statistical parameters including central tendency (e.g. means) or other basic estimates (e.g. regression coefficient) AND variation (e.g. standard deviation) or associated estimates of uncertainty (e.g. confidence intervals)
☐	☒	For null hypothesis testing, the test statistic (e.g. *F*, *t*, *r*) with confidence intervals, effect sizes, degrees of freedom and *P* value noted *Give P values as exact values whenever suitable.*
☒	☐	For Bayesian analysis, information on the choice of priors and Markov chain Monte Carlo settings
☒	☐	For hierarchical and complex designs, identification of the appropriate level for tests and full reporting of outcomes
☐	☒	Estimates of effect sizes (e.g. Cohen's *d*, Pearson's *r*), indicating how they were calculated

Our web collection on statistics for biologists contains articles on many of the points above.

Software and code

Policy information about availability of computer code

Data collection	Gen5 Microplate Reader and Imager Software V3.05 (BioTek), BD FACSDiva V8.0.2, NIS-Elements AR4.50.00 software (Nikon)
Data analysis	Fiji v.2.0.0-rc-68/1.52h, fetchMG V1.0, ete3 toolkit V3.1.1, ClustralOmega V1.2.4, IQTree V1.5.5, DADA2 V1.18.0 & V1.8.0, MAPseq V1.2.3, hpc-clust V1.2.1, Infernal V1.1.2, DESeq2 V1.32.0, (see references in manuscript). GraphPad Prism 8, FlowJo V.10.3 (Treestar), R (version 3.4.2). MassHunter Qualitative Analysis Software (Agilent Technologies, version 10.0) Custom code is available at https://git.embl.de/maier/abxbug

For manuscripts utilizing custom algorithms or software that are central to the research but not yet described in published literature, software must be made available to editors and reviewers. We strongly encourage code deposition in a community repository (e.g. GitHub). See the Nature Research guidelines for submitting code & software for further information.

Data

Policy information about availability of data

All manuscripts must include a data availability statement. This statement should provide the following information, where applicable:

- Accession codes, unique identifiers, or web links for publicly available datasets
- A list of figures that have associated raw data
- A description of any restrictions on data availability

Data is available from Zenodo: http://doi.org/10.5281/zenodo.3527540, EUCAST database: https://eucast.org/clinical_breakpoints/

Field-specific reporting

Please select the one below that is the best fit for your research. If you are not sure, read the appropriate sections before making your selection.

☒ Life sciences ☐ Behavioural & social sciences ☐ Ecological, evolutionary & environmental sciences

For a reference copy of the document with all sections, see nature.com/documents/nr-reporting-summary-flat.pdf

Life sciences study design

All studies must disclose on these points even when the disclosure is negative.

Sample size	For animals experiments: Power Analysis using G*Power. For stool-derived communities, microbiome analysis was an exploratory analysis for which a meaningful power analysis could not be performed a priori. For experiments other than animal studies, no prior assumptions were made regarding sample size.
Data exclusions	Replicates with pre-established inconsistent growth behavior were excluded from our analysis (for details please see "Methods")
Replication	We have three to five biological replicates for each strain in the Prestwick library screen and two to three biological replicates for the MICs. For the antidote screen, we have two biological replicates. Checkerboards were performed in two to four biological replicates. All other experiments were performed in at least three independent replicates. All attempts at replication were successful.
Randomization	human-stool derived communities: stool from all donors were used for all experimental groups (untreated, antibiotic-treated, antibiotic + antidote treated). Thus, randomization was not relevant to our study. animal experiments: animals were randomly allocated to experimental groups.
Blinding	For in vitro experiments, no blinding was performed, since it was necessary to keep track of which samples are used in each experiment. Controls were always processed in parallel. For animal experiments, analysis of fecal drug concentration was blinded.

Reporting for specific materials, systems and methods

We require information from authors about some types of materials, experimental systems and methods used in many studies. Here, indicate whether each material, system or method listed is relevant to your study. If you are not sure if a list item applies to your research, read the appropriate section before selecting a response.

Materials & experimental systems

n/a	Involved in the study	
☒	☐	Antibodies
☒	☐	Eukaryotic cell lines
☒	☐	Palaeontology and archaeology
☐	☒	Animals and other organisms
☐	☒	Human research participants
☒	☐	Clinical data
☒	☐	Dual use research of concern

Methods

n/a	Involved in the study	
☒	☐	ChIP-seq
☐	☒	Flow cytometry
☒	☐	MRI-based neuroimaging

Animals and other organisms

Policy information about studies involving animals; ARRIVE guidelines recommended for reporting animal research

Laboratory animals	Gnotobiotic C57BL/6J mice that were stably colonized with 12-community member consortium, female and male mice between 6-12 weeks. Housing conditions: 22 +/- 1.5°C, 50 +/- 5% humidity, 12-hour light/ 12-hour dark cycle.
Wild animals	The study did not involve wild animals.
Field-collected samples	The study did not involve samples collected from the field.
Ethics oversight	Regierung von Oberbayern, ROB-55.2-2532.Vet_02-17-120

Note that full information on the approval of the study protocol must also be provided in the manuscript.

Human research participants

Policy information about studies involving human research participants

Population characteristics	The study was only open to participants that have, to the best of their knowledge, a healthy gut

Population characteristics	microbiota. The participants should not have taken any antibiotics for 12 months prior to sample donation, and should not have been diagnosed with any disease related to the intestinal microbiota. These include inflammatory bowel disease, colon cancer, lactose intolerance, diabetes as well as recently experienced diarrhoea. The study was open to all genders and age groups.
Recruitment	staff at EMBL Heidelberg: the sample processing procedure requires the participants to provide their faecal sample within minutes after collection, which therefore had to occur at EMBL Heidelberg. All participants therefore work at the same workplace and eat at the same canteen, which might impact overall microbiome composition of the participants.
Ethics oversight	EMBL Bioethics Internal Advisory Committee (BIAC2015-009 Rev.3, approved on June 3rd, 2016)

Note that full information on the approval of the study protocol must also be provided in the manuscript.

Flow Cytometry

Plots

Confirm that:

☒ The axis labels state the marker and fluorochrome used (e.g. CD4-FITC).

☒ The axis scales are clearly visible. Include numbers along axes only for bottom left plot of group (a 'group' is an analysis of identical markers).

☒ All plots are contour plots with outliers or pseudocolor plots.

☒ A numerical value for number of cells or percentage (with statistics) is provided.

Methodology

Sample preparation	cells were live/dead stained using the LIVE/DEAD BacLight Bacterial viability and counting kit (#L34856 Molecular Probes, ThermoFisher) according to the manufacturer's protocol before and after antibiotic treatment.
Instrument	BD LSRFortessaTM flow cytometer
Software	Graphs were generated using the FlowJo V10.3 software (Treestar)
Cell population abundance	Flow cytometry analysis of bacterial cells.
Gating strategy	The forward and side scatter signals (488 nm) as well as the green and red fluorescent signals (488-530/30A filter and 561-610/20A filter, respectively) were acquired. The FSC/SSC detectors were set to logarithmic scale. Gating strategy as previously described for bacterial populations and as recommended by the kit. The flow rate varied between 12 µl/min and 60 µl/min depending on the concentration of each sample, and the analysis was stopped when 10,000 target events were measured.

☒ Tick this box to confirm that a figure exemplifying the gating strategy is provided in the Supplementary Information.